Joint 21st AIRAPT and 45th EHPRG

New pressure-induced photoluminescence phenomena in Mn^{2+} and Cr^{3+} materials

Ignacio Hernández and Fernando Rodríguez

Catania, 17th-21th Sept., 2007

Joint 21st AIRAPT and 45th EHPRG

New pressure-induced photoluminescence phenomena in Mn^{2+} and Cr^{3+} materials

Ignacio Hernández and Fernando Rodríguez

Queen Mary
University of London

Catania, 17th-21th Sept., 2007

Outline.

- Motivation.Objectives
- Strategies. Experimental
- Results
    - Fluorites (MF_2: Mn^{2+}, M=Ca, Sr, Ba)
    - Elpasolites (A_2BMF_6: Cr^{3+}, A= Rb,K,Tl; B=Na,K; M=Ga, In, Cr)
    - MnF_2
- Conclusions

Motivation.

- Transition Metal Ions: Cr^{3+}, Ti^{3+}, Mn^{2+},...

- Luminescent devices: **lasers**, scintillators, organic,... ☺
- Usually impurities 😐
- Pure materials are usually not luminescent at RT ☹
- Pure or concentrated would provide more emission ☺

- No general rule to predict *a priori* wheter a material will be luminescent or not ☹

- No general rule to predict accurately the optical (in particular photoluminescence) spectrum ☹

Objectives.

Introduction

Twofold aim:

1- Study of the mechanisms governing photoluminescence (PL) in transition-metal ions.

- ● Non-radiative de-excitation in impurities
- ■ Non-radiative de-excitation in concentrated materials
- ◆ Structure-spectra correlations

2- Induction of new PL phenomena.

- ✸ Photoluminescence at low temperature or room temperature.
- ✸ Spectrum transformations. Changes in electronic configuration.

Strategies.

Correlations between optical phenomena and structure

- ● Impurities: PL in $Ca_{1-x}Sr_xF_2$: Mn^{2+} and BaF_2: Mn^{2+}
  - Temperature dependence
  - Pressure experiments
- ■ Pure transition-metal ions: MnF_2
  - Single-crystal pressure experiments
  - Effect of grain size reduction (milling)
- ◆ Spectrum-structure corr.: A_2BMF_6 : Cr^{3+} fluoroelpasolites
  - Structural and optical characterization (correlations)
  - Pressure experiments

Introduction

Experimental.

Adaptation of spectroscopic techniques to high pressure.

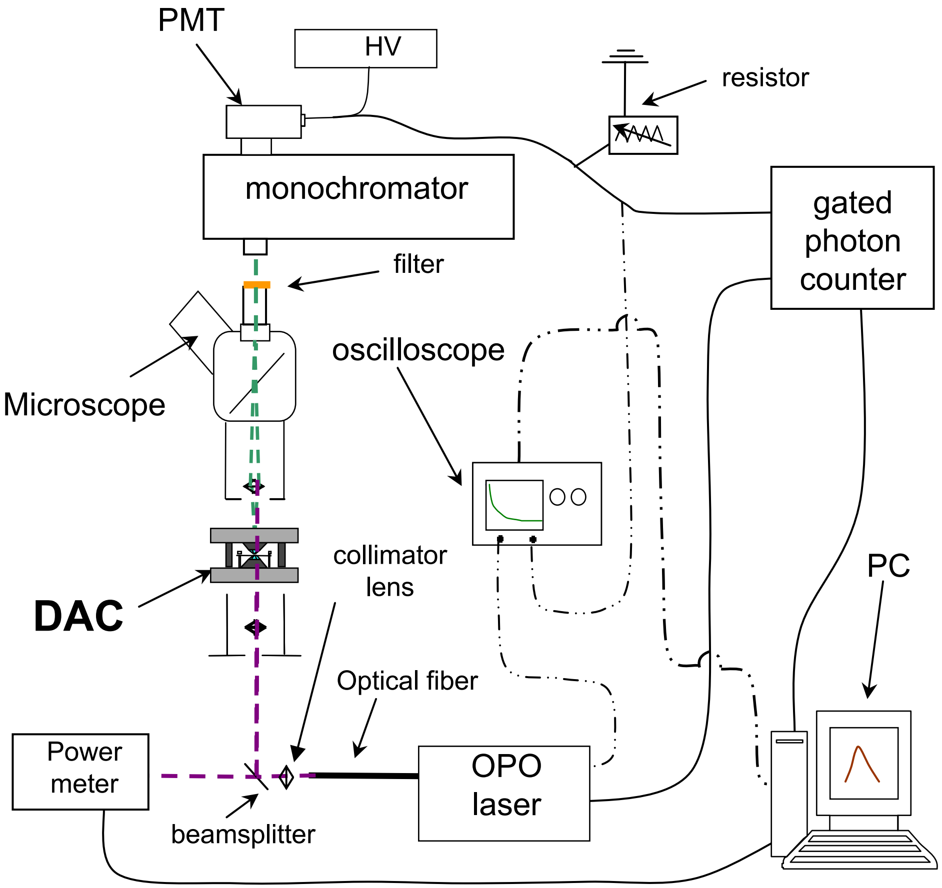

Experimental.

Introduction

Adaptation of spectroscopic techniques to high pressure.

- Time resolved
- Emission
- Excitation
- PL lifetime
- (Absorption)

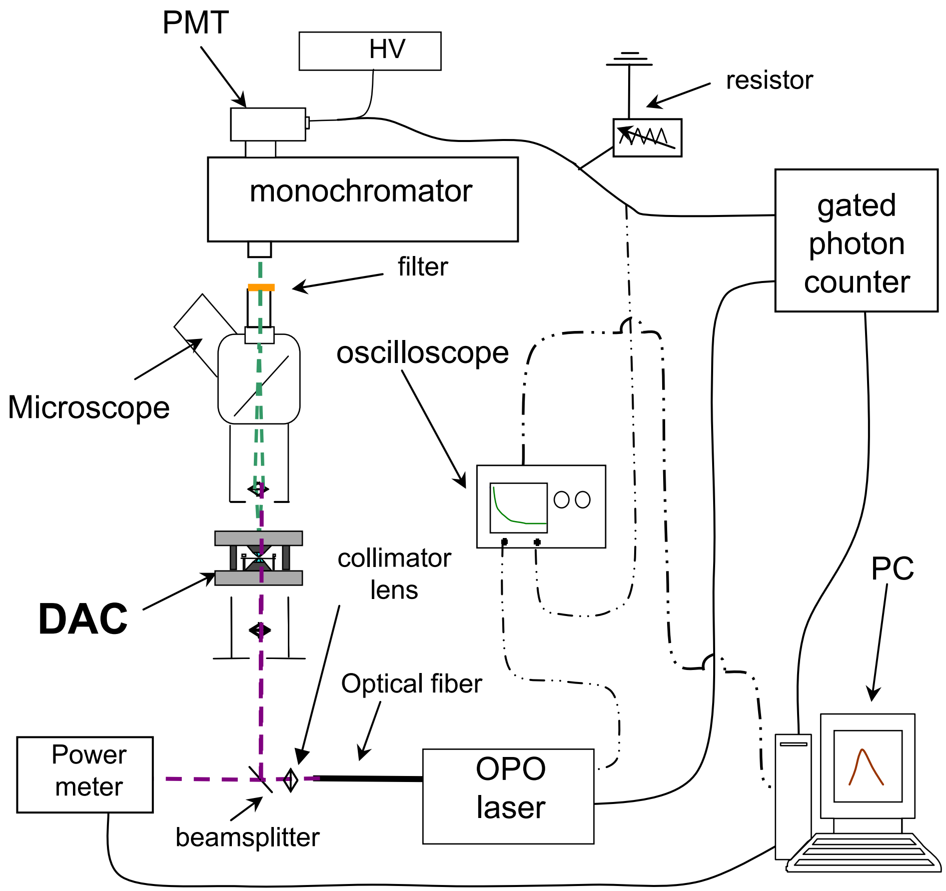

$Ca_{1-x}Sr_xF_2$: Mn^{2+} and BaF_2: Mn^{2+} Fluorites

Non-radiative phenomena in impurity systems

Crystal field states for transition-metal ions.

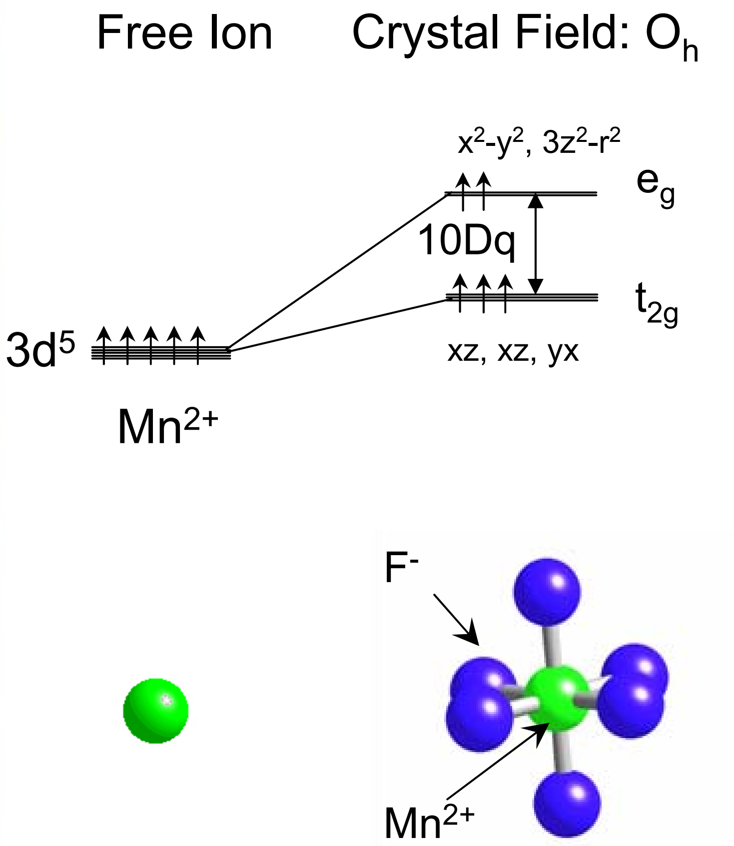

Tanabe-Sugano Diagram

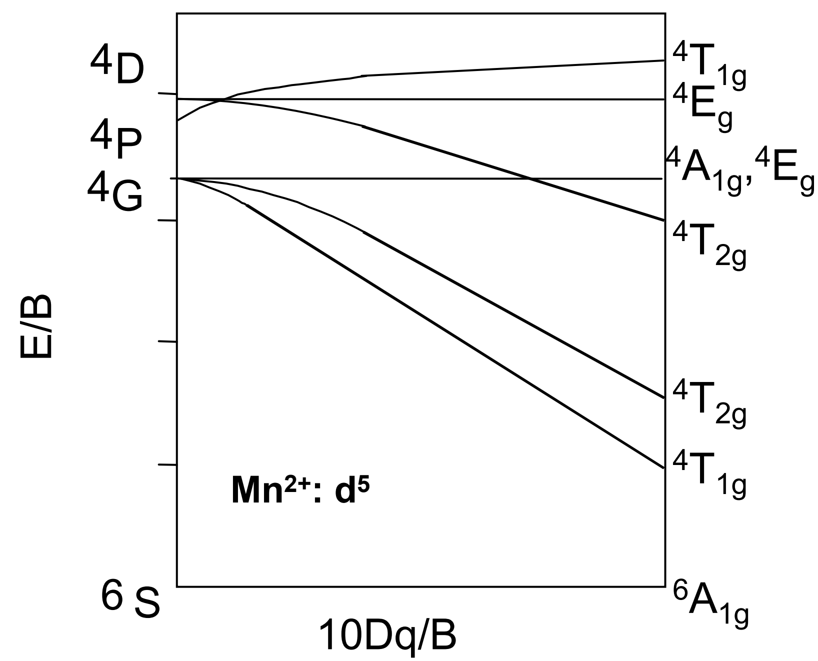

Phenomenological model

$Ca_{1-x}Sr_xF_2$: Mn^{2+} band structure.

$Ca_{1-x}Sr_xF_2$: Mn^{2+}

Cubal (hexahedral) symmetry

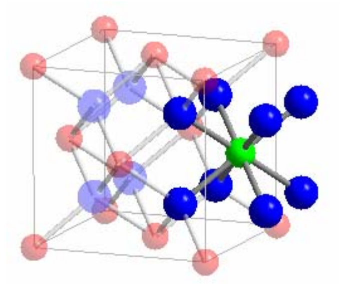

unlike ABF_3: Mn^{2+} perovskites: octahedral <MnF_2 (q-oct)>

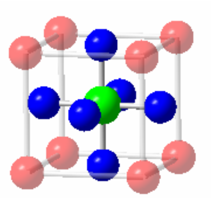

Mn^{2+} (d^{5+})

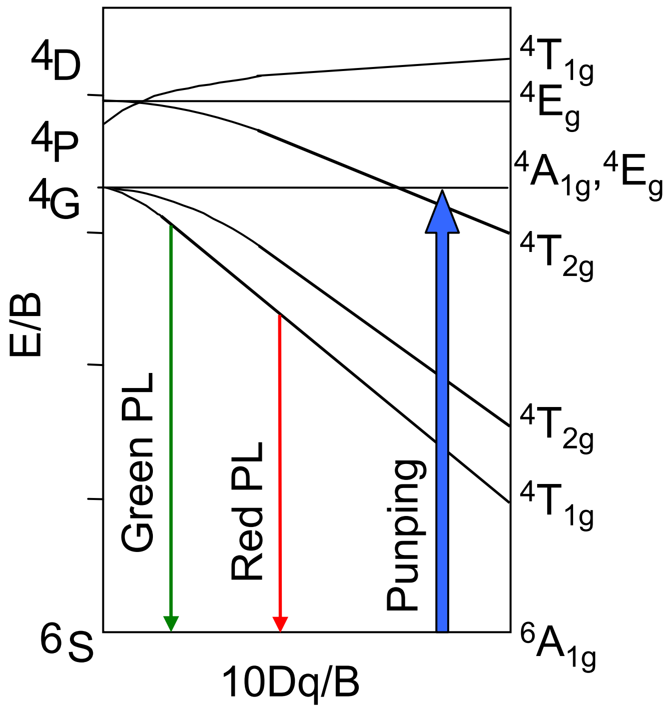

$10Dq(ML_8) < 10Dq\ (ML_6)$

$[10Dq(ML_8) \approx 1/2\ 10Dq(ML_6)]$

Higher gap → smaller non-radiative transition probability.

$Ca_{1-x}Sr_xF_2$: Mn^{2+} PL variations along the series at RT.

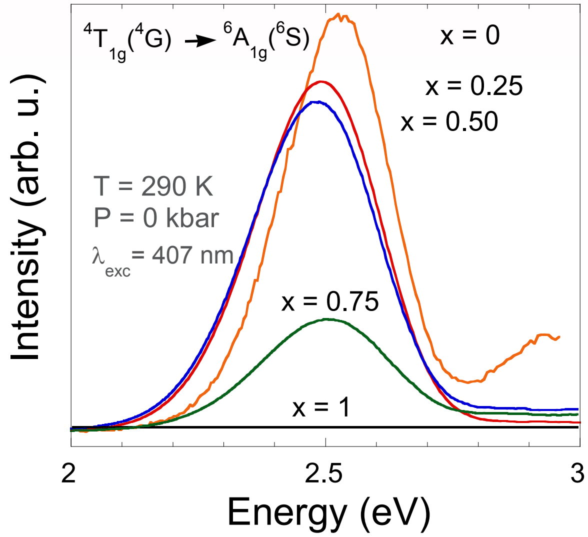

PL at room temperature disappears along the series for x > 0.75

SrF_2: Mn^{2+} is not PL at RT

$Ca_{1-x}Sr_xF_2$: Mn^{2+} PL variations along the series at RT.

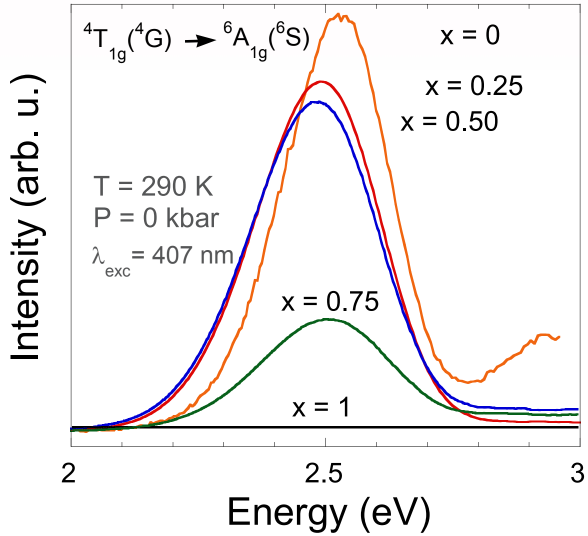

PL at room temperature disappears along the series for x > 0.75

SrF_2: Mn^{2+} is not PL at RT

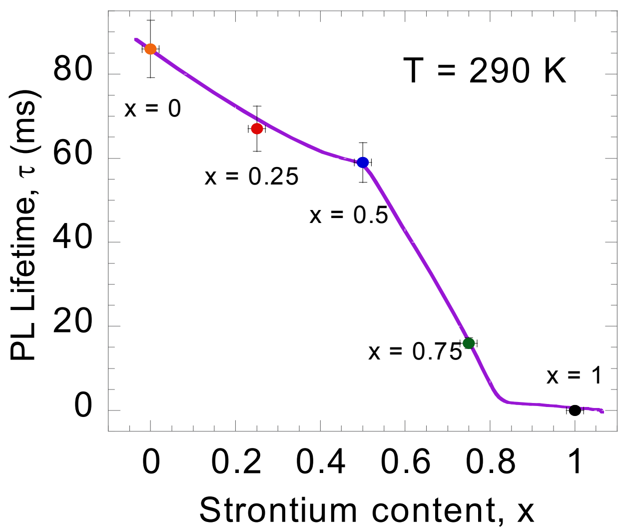

Strong correlation between the PL Intensity and PL Lifetime

Drop for x > 0.5

Multiphonon non-radiative processes

Results - Fluorites

$Ca_{1-x}Sr_xF_2$: Mn^{2+} PL variations with temperature

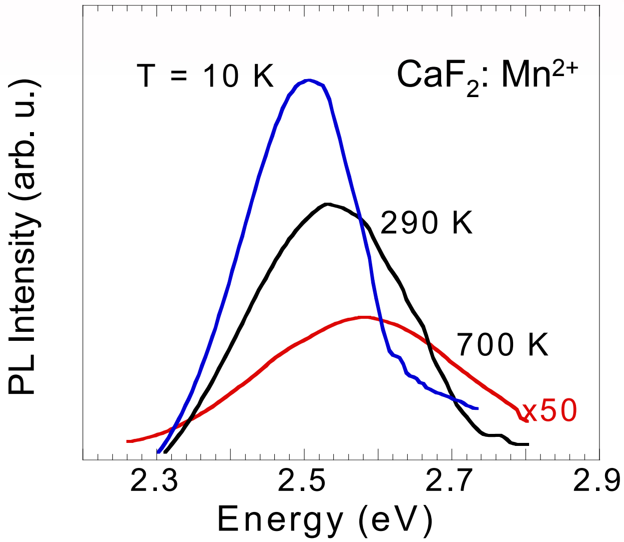

PL disappears upon T ↑

Similar behaviour for all the crystals

$T_{quenching}$ ↓ with Strontium content ↑

Results - Fluorites

$Ca_{1-x}Sr_xF_2$: Mn^{2+} PL variations with temperature

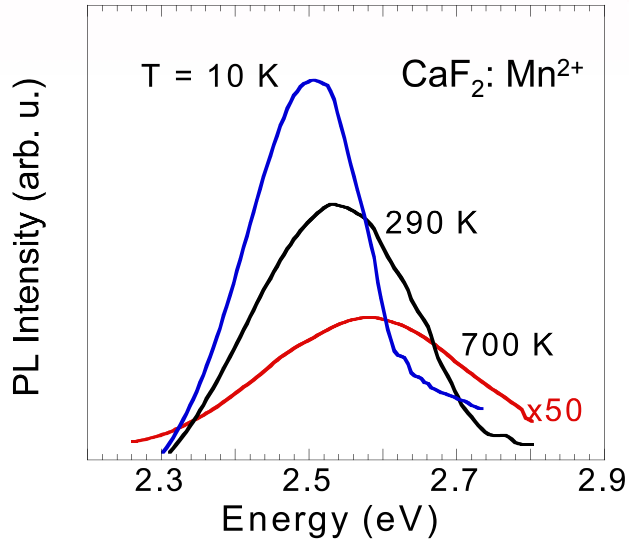

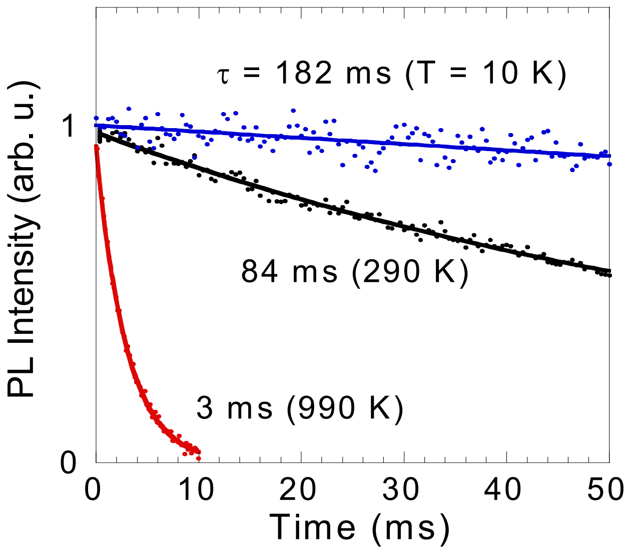

PL disappears upon T ↑

Similar behaviour for all the crystals

$T_{quenching}$ ↓ with Strontium content ↑

Correlation between I and τ

Non-radiative de-excitation processes thermal activation

Dexter-Klick-Russell model. Spectroscopic study.

$Ca_{1-x}Sr_xF_2$: Mn^{2+}

Dexter-Klick-Russell criterion for the absence of PL

$$\Lambda = \frac{1}{2}\frac{E_{abs} - E_{em}}{E_{abs}} = \frac{1}{2}\frac{\Delta E_{stokes}}{E_{abs}}$$

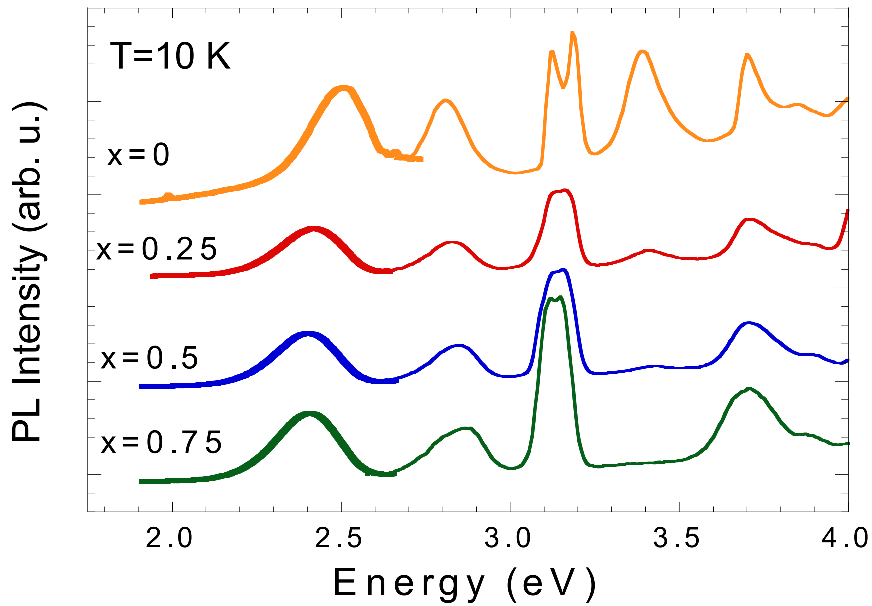

Results - Fluorites

Dexter-Klick-Russell model. Spectroscopic study.

$Ca_{1-x}Sr_xF_2: Mn^{2+}$

Dexter-Klick-Russell criterion for the absence of PL

$$\Lambda = \frac{1}{2}\frac{E_{abs} - E_{em}}{E_{abs}} = \frac{1}{2}\frac{\Delta E_{stokes}}{E_{abs}}$$

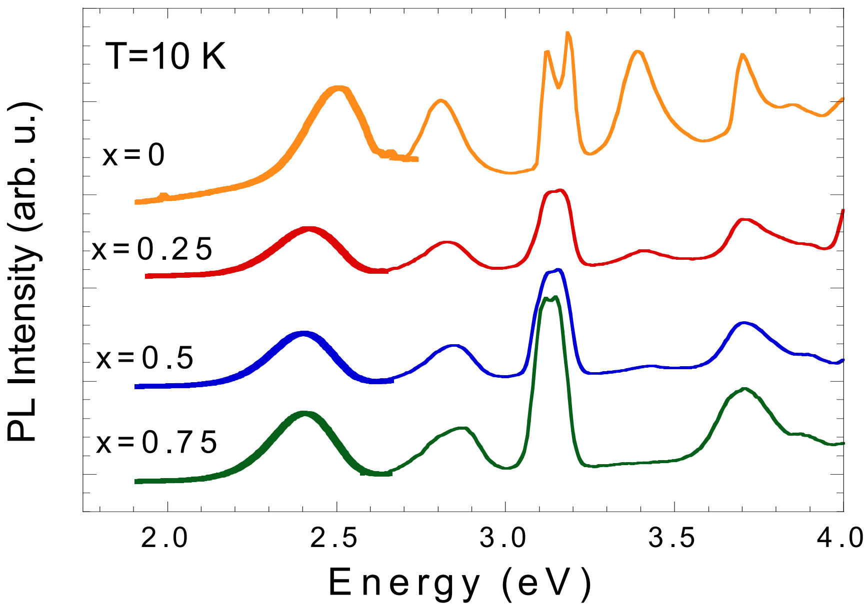

Very low Λ with no physical meaning

No significant correlations E_{em}, E_{abs}, ΔE_{Stokes} vs. x

Dexter-Klick-Russell model. Spectroscopic study.

Results - Fluorites

$Ca_{1-x}Sr_xF_2$: Mn^{2+}

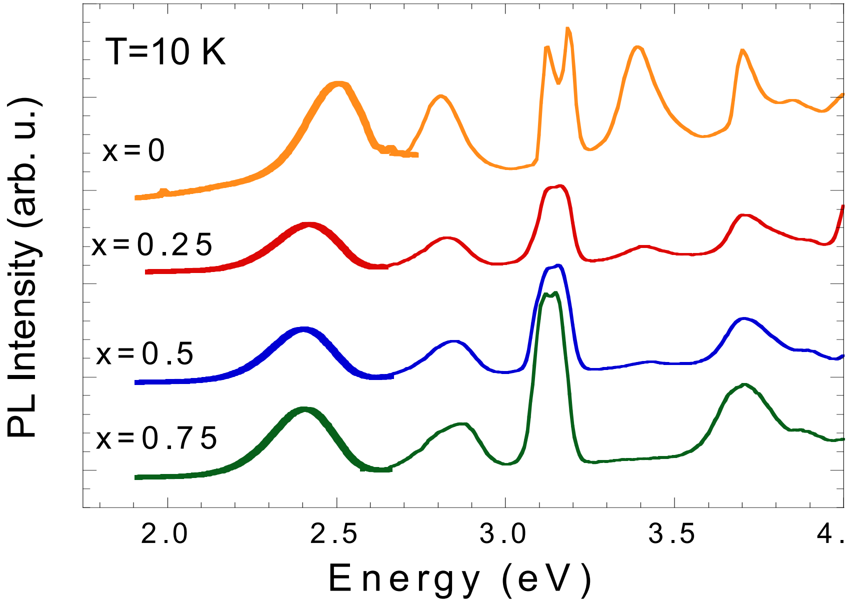

Dexter-Klick-Russell criterion for the absence of PL

$$\Lambda = \frac{1}{2}\frac{E_{abs} - E_{em}}{E_{abs}} = \frac{1}{2}\frac{\Delta E_{stokes}}{E_{abs}}$$

$$\tau_{nr}^{-1} = p \cdot e^{-\frac{E_a}{KT}}$$

Very low Λ with no physical meaning

No significant correlations E_{em}, E_{abs}, ΔE_{Stokes} vs. x

Intensity quenching. Activation energy, E_a.

$Ca_{1-x}Sr_xF_2$: Mn^{2+}

$$\eta = \frac{\tau_{rad}^{-1}}{\tau_{rad}^{-1} - \tau_{nr}^{-1}} = \frac{1}{1 + A \cdot e^{-\frac{E_a}{KT}}}$$

$$\Rightarrow \quad I_{PL}(T) = I_{PL}(0) \cdot \eta(T)$$

Intensity quenching. Activation energy, E_a.

$Ca_{1-x}Sr_xF_2$: Mn^{2+}

$$\eta = \frac{\tau_{rad}^{-1}}{\tau_{rad}^{-1} - \tau_{nr}^{-1}} = \frac{1}{1 + A \cdot e^{-\frac{E_a}{KT}}}$$

$$\Rightarrow \quad I_{PL}(T) = I_{PL}(0) \cdot \eta(T)$$

$$\ln[I_{PL}(T)^{-1} - I_{PL}(0)^{-1}] \quad \text{vs.} \quad 1/T \quad \rightarrow \quad E_a$$

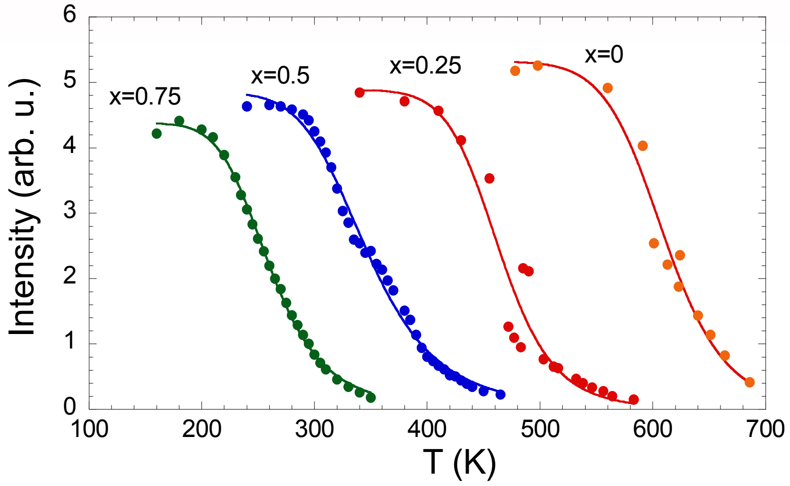

Results - Fluorites

Intensity quenching. Activation energy, E_a.

$Ca_{1-x}Sr_xF_2$: Mn^{2+}

$$\eta = \frac{\tau_{rad}^{-1}}{\tau_{rad}^{-1} - \tau_{nr}^{-1}} = \frac{1}{1 + A \cdot e^{-\frac{E_a}{KT}}}$$

$$\Rightarrow \quad I_{PL}(T) = I_{PL}(0) \cdot \eta(T)$$

$$\ln[I_{PL}(T)^{-1} - I_{PL}(0)^{-1}] \quad \text{vs.} \quad 1/T \quad \rightarrow \quad E_a$$

x	Activation energy, E_a		
0	12500 K	8680 cm^{-1}	1.08 eV
0.25	7400 K	5140 cm^{-1}	0.64 eV
0.5	4800 K	3330 cm^{-1}	0.41 eV
0.75	3500 K	2430 cm^{-1}	0.30 eV

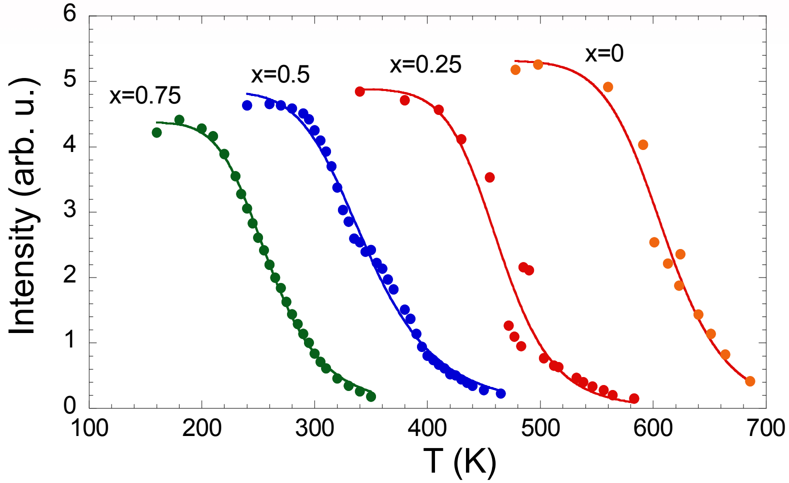

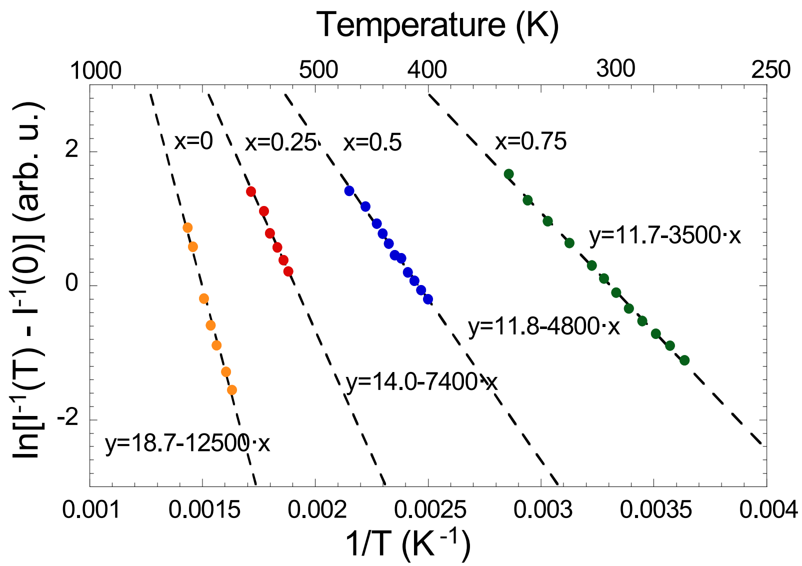

PL Lifetime: E_a and p.

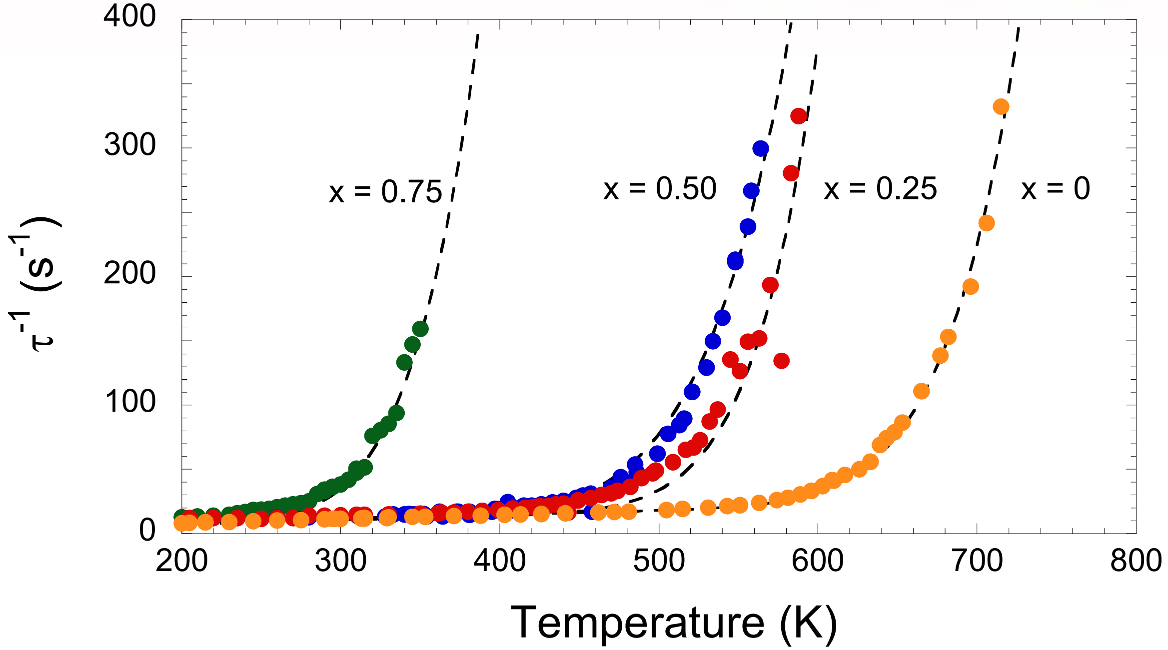

$$\tau^{-1}(T) = \underbrace{\tau_0^{-1} + \tau_{ED}^{-1}\,\mathrm{Coth}\frac{\hbar\omega_u}{2k_B T}}_{\textbf{rad}} + \underbrace{p \cdot e^{-\frac{E_a}{k_B T}}}_{\textbf{nr}}$$

PL Lifetime: E_a and p.

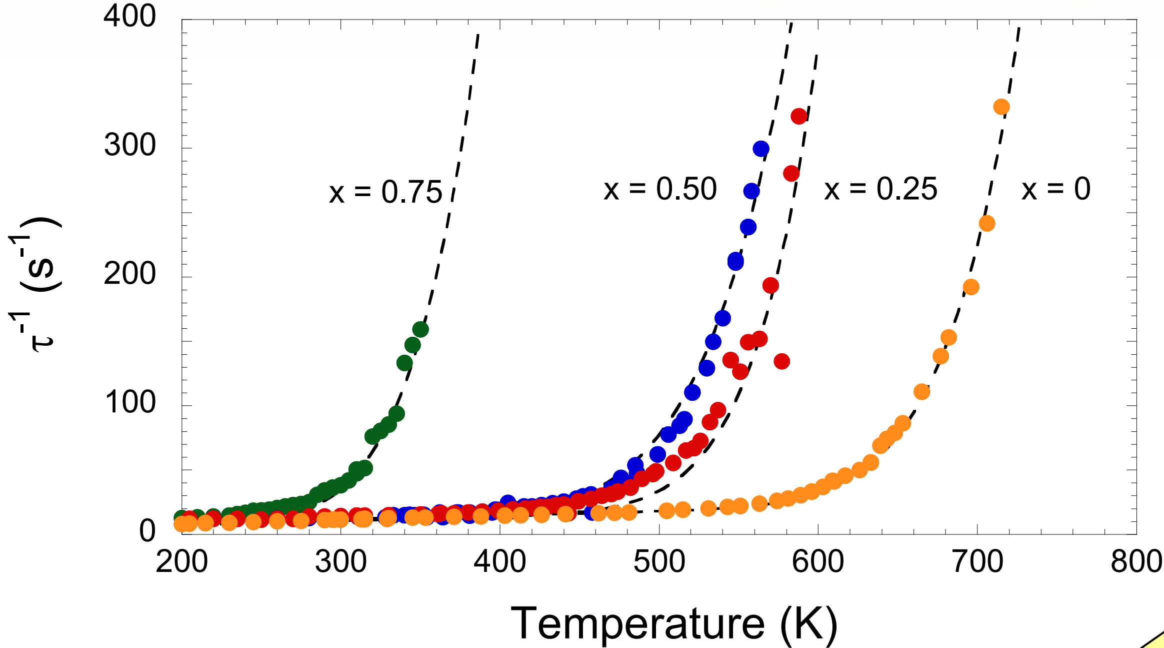

$$\tau^{-1}(T) = \underbrace{\tau_0^{-1} + \tau_{ED}^{-1}\mathrm{Coth}\frac{\hbar\omega_u}{2k_BT}}_{\textbf{rad}} + \underbrace{p \cdot e^{-\frac{E_a}{k_BT}}}_{\textbf{nr}}$$

x	Pre-exponential rate, p	Activation energy, E_a	
0	$4.2\text{x}10^9$ s^{-1}	8130 cm^{-1}	1.01 eV
0.25	$1.4\text{x}10^9$ s^{-1}	6670 cm^{-1}	0.83 eV
0.5	$2.1\text{x}10^7$ s^{-1}	5530 cm^{-1}	0.69 eV
0.75	$4.2\text{x}10^6$ s^{-1}	2750 cm^{-1}	0.34 eV

Variation of E_a and p with x or *a*.

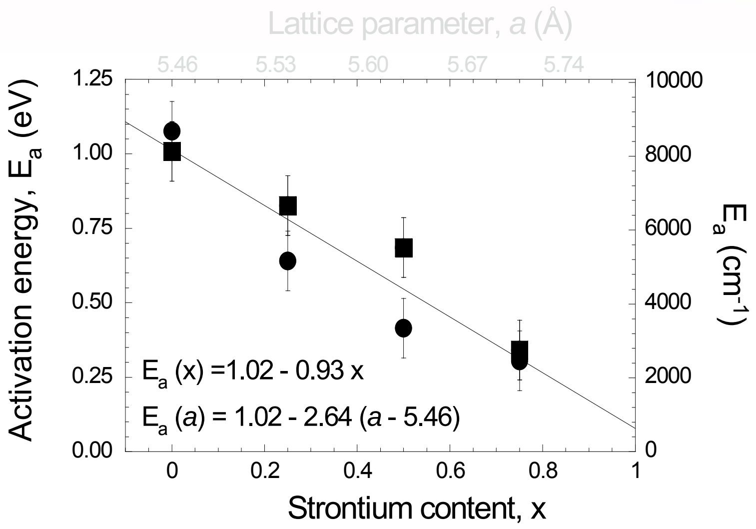

Results - Fluorites

Variation of E_a and p with x or *a*.

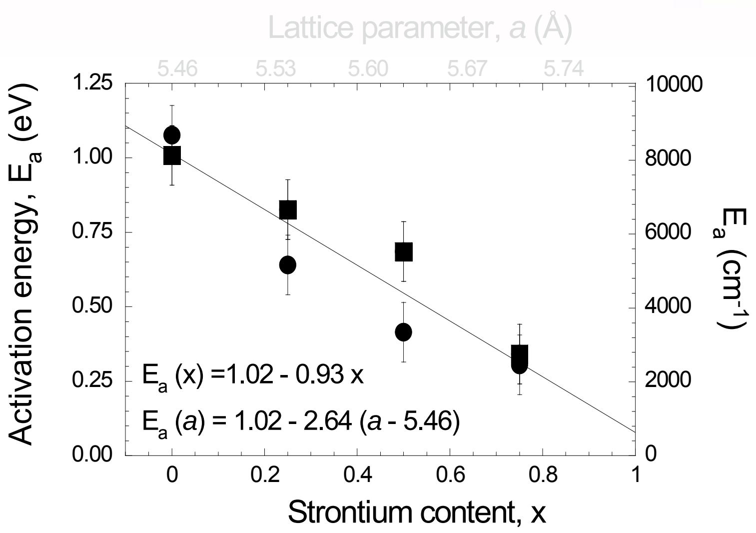

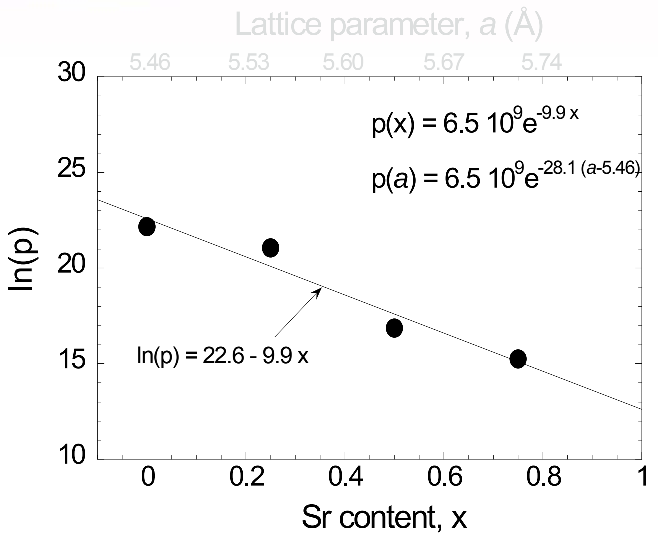

$$\frac{\Delta w_{nr}(p,E_a)}{w_{nr}} = \frac{\Delta p}{p} - \frac{\Delta E_a}{k_B T} = -28\Delta p - \frac{\Delta E_a}{k_B T}$$

Results - Fluorites

Variation of E_a and p with x or *a*.

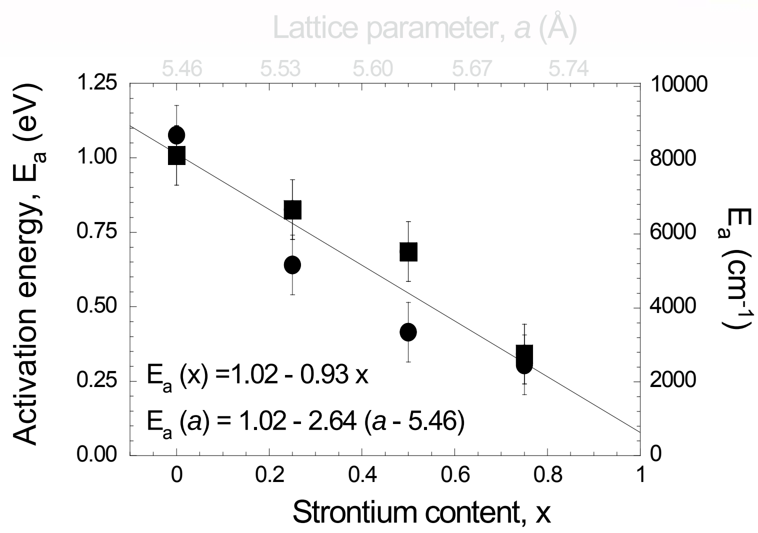

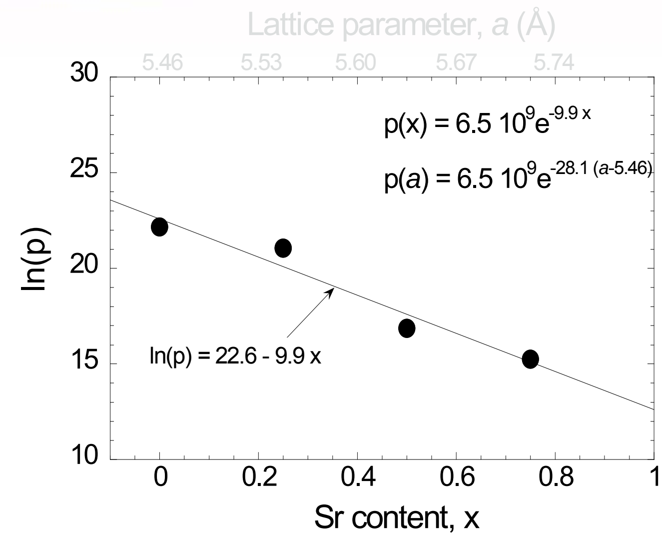

$$\frac{\Delta w_{nr}(p,E_a)}{w_{nr}} = \frac{\Delta p}{p} - \frac{\Delta E_a}{k_B T} = -28\Delta p - \frac{\Delta E_a}{k_B T}$$

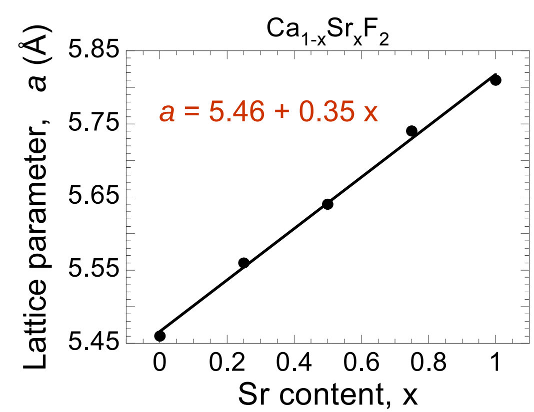

Results - Fluorites

Variation of E_a and p with x or *a*.

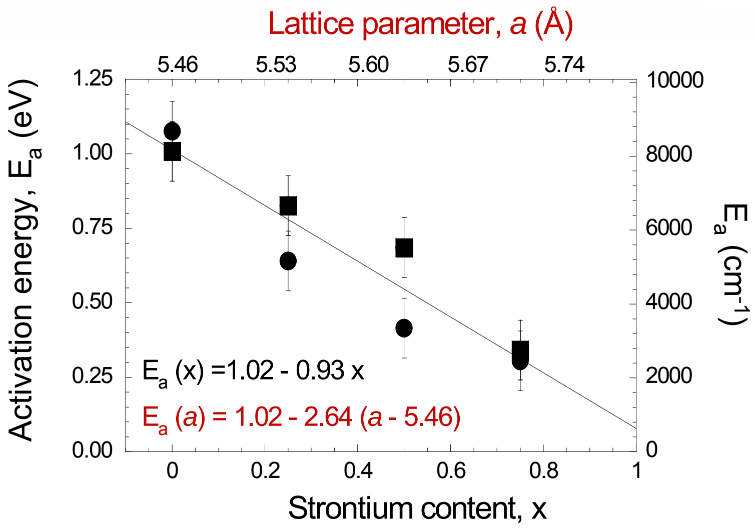

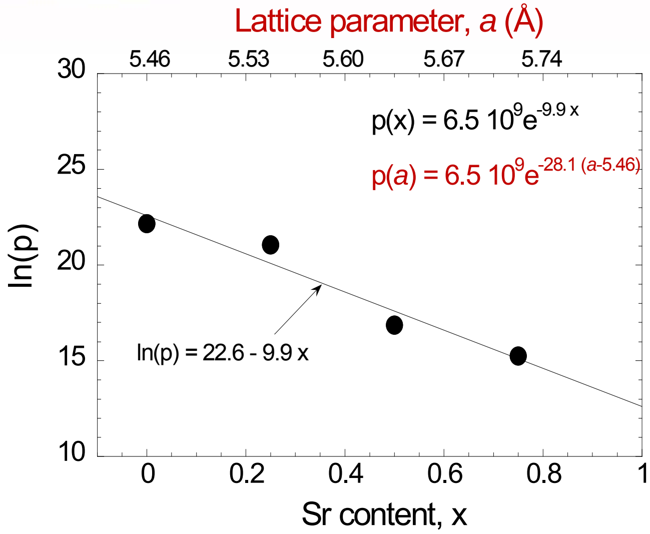

$$\frac{\Delta w_{nr}(p,E_a)}{w_{nr}} = \frac{\Delta p}{p} - \frac{\Delta E_a}{k_B T} = -28\Delta p - \frac{\Delta E_a}{k_B T}$$

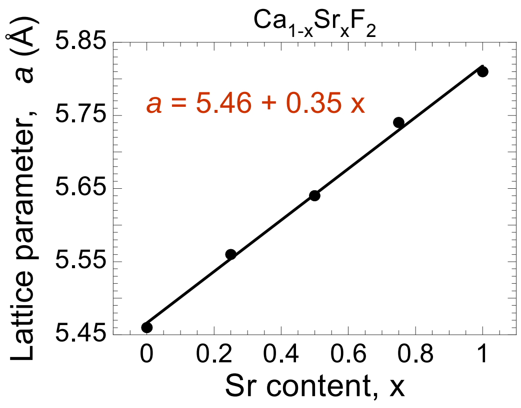

Variation of E_a and p with x or *a*.

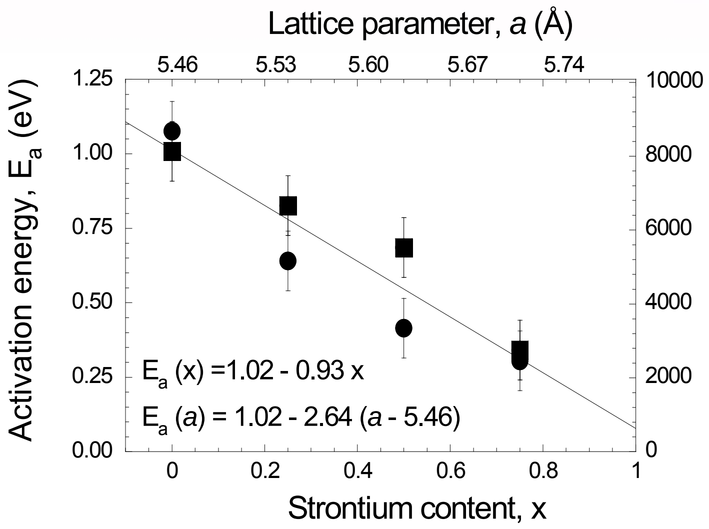

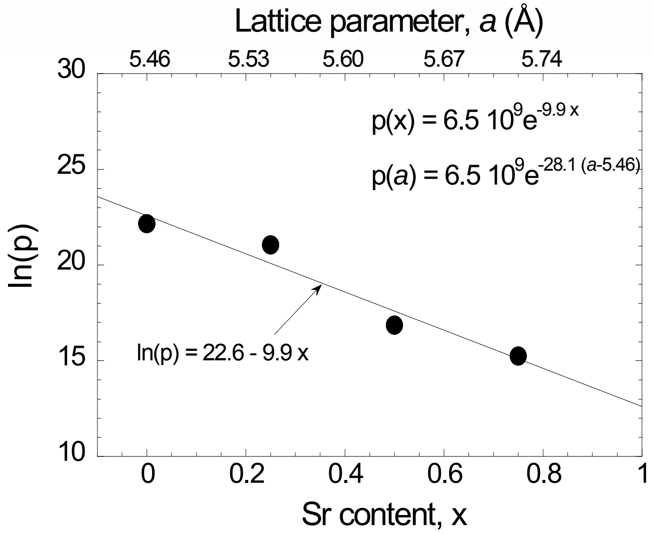

$$\frac{\Delta w_{nr}(p,E_a)}{w_{nr}} = \frac{\Delta p}{p} - \frac{\Delta E_a}{k_B T} = -28\Delta p - \frac{\Delta E_a}{k_B T}$$

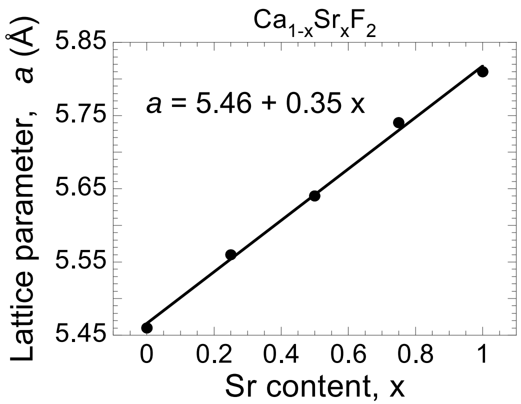

Are NR processes due to the different composition?

or are they a pure volume effect?

$Ca_{0.5}Sr_{0.5}F_2$: Mn^{2+}. Pressure results.

$Ca_{0.5}Sr_{0.5}F_2$: Mn^{2+}. Pressure results.

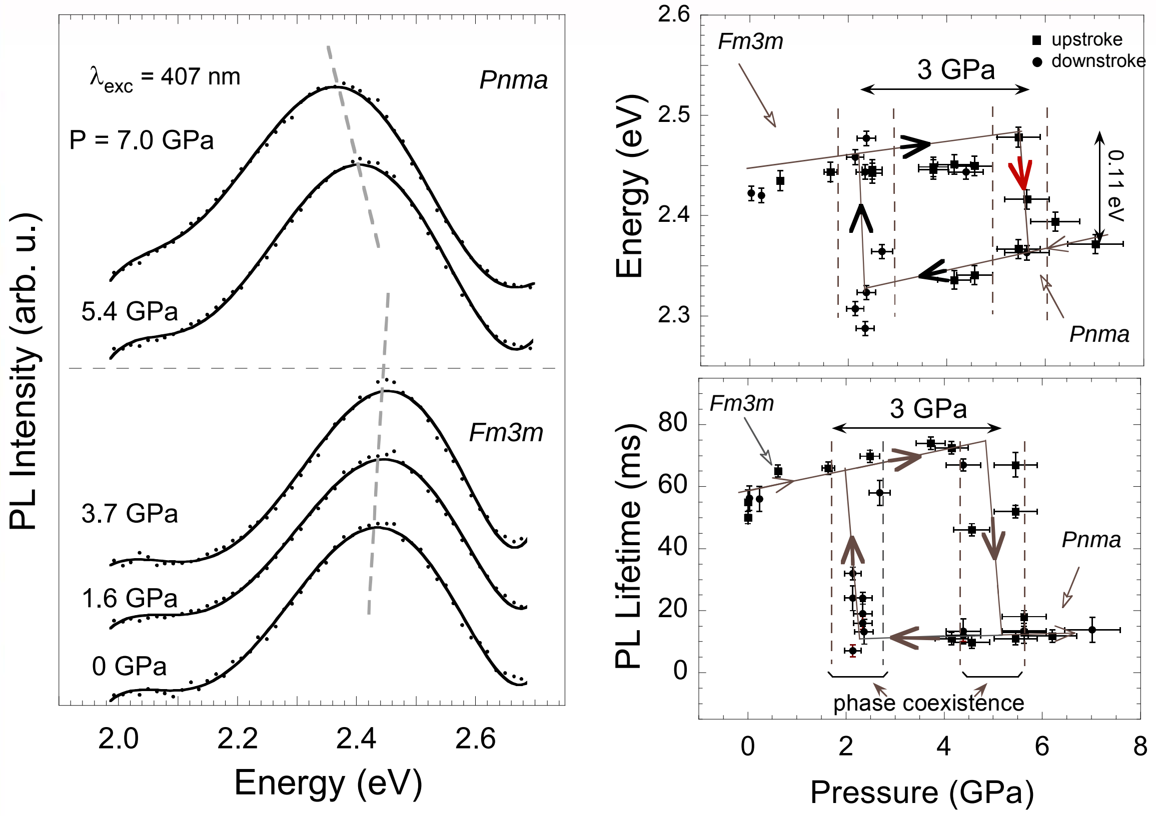

Abrupt redshift

Abrupt τ decrease

Hysteresis

Phase Transition effect: fluorite-to-cotunnite

Phase-transition sequence.

Fluorite

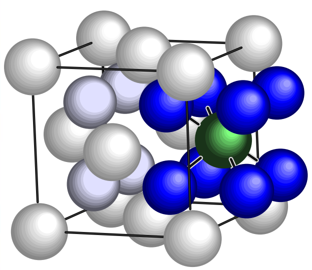

Cotunnite (α-$PbCl_2$)

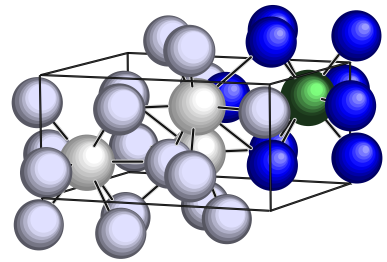

~10 % Volume reduction

CaF_2	8.0 GPa
SrF_2	5.2 GPa
BaF_2	1.7 Gpa

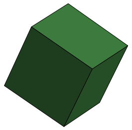

Cubal symmetry

Eightfold coordination

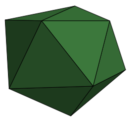

Non-centrosymmetric

Ninefold coordination

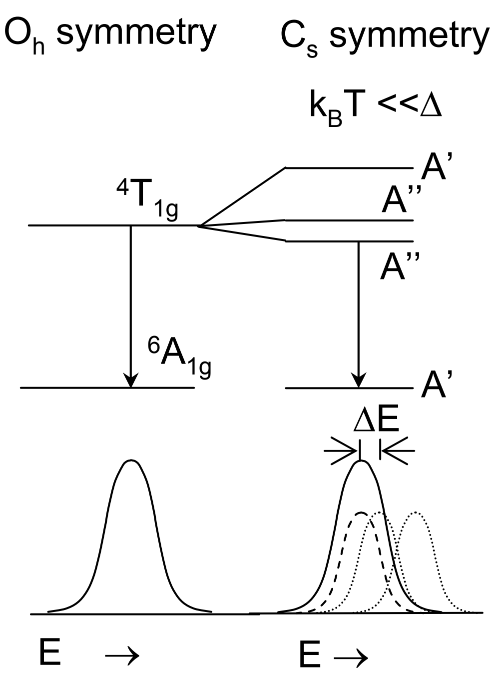

$Ca_{0.25}Sr_{0.75}F_2$: Mn^{2+}. Pressure results.

Results - Fluorites

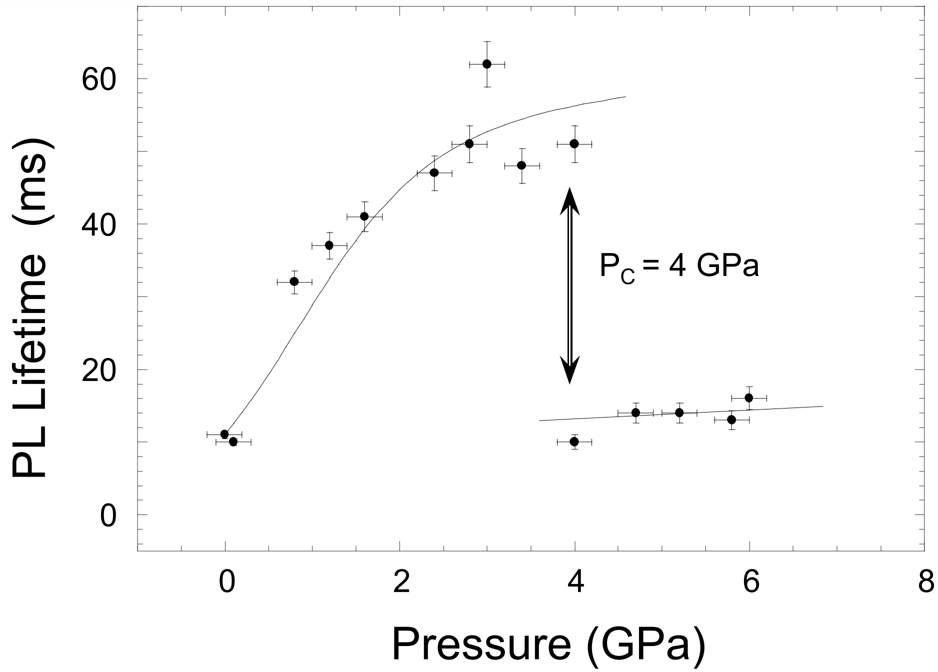

Pressure-induced PL enhancement

τ ~ 12 ms $\rightarrow$ τ ~ 60 ms from P = 0 GPa to P ~ 4 GPa

Can we recover PL in non-PL systems?

SrF_2: Mn^{2+} and BaF_2: Mn^{2+} under pressure.

SrF_2: Mn^{2+}

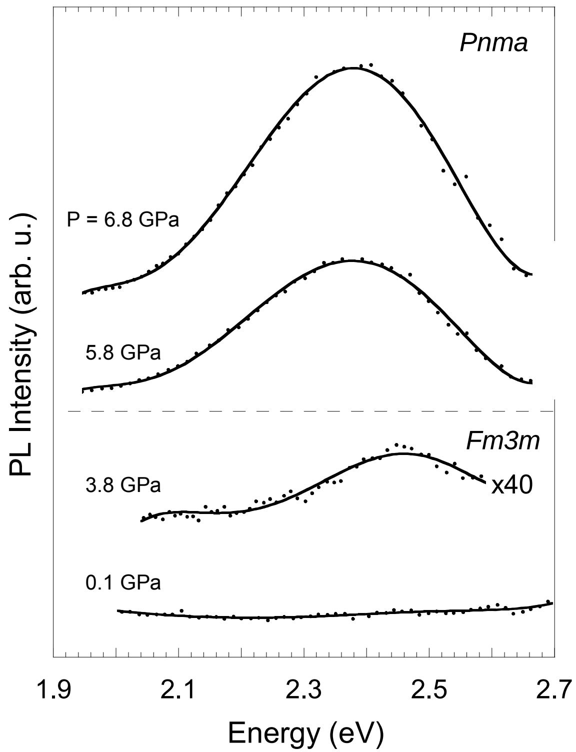

BaF_2: Mn^{2+}

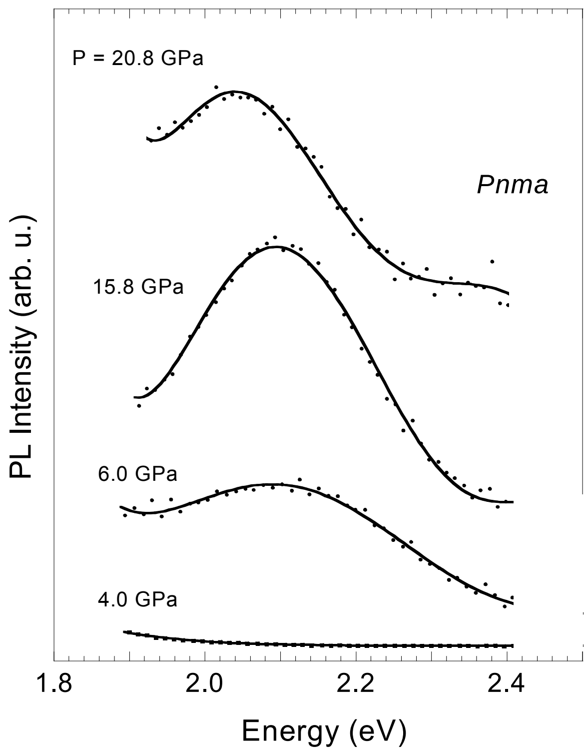

PL appearance in the fluorite phase & PL enhancement in the cotunnite phase

PL in the cotunnite phase!!!

General behaviour.

Results - Fluorites

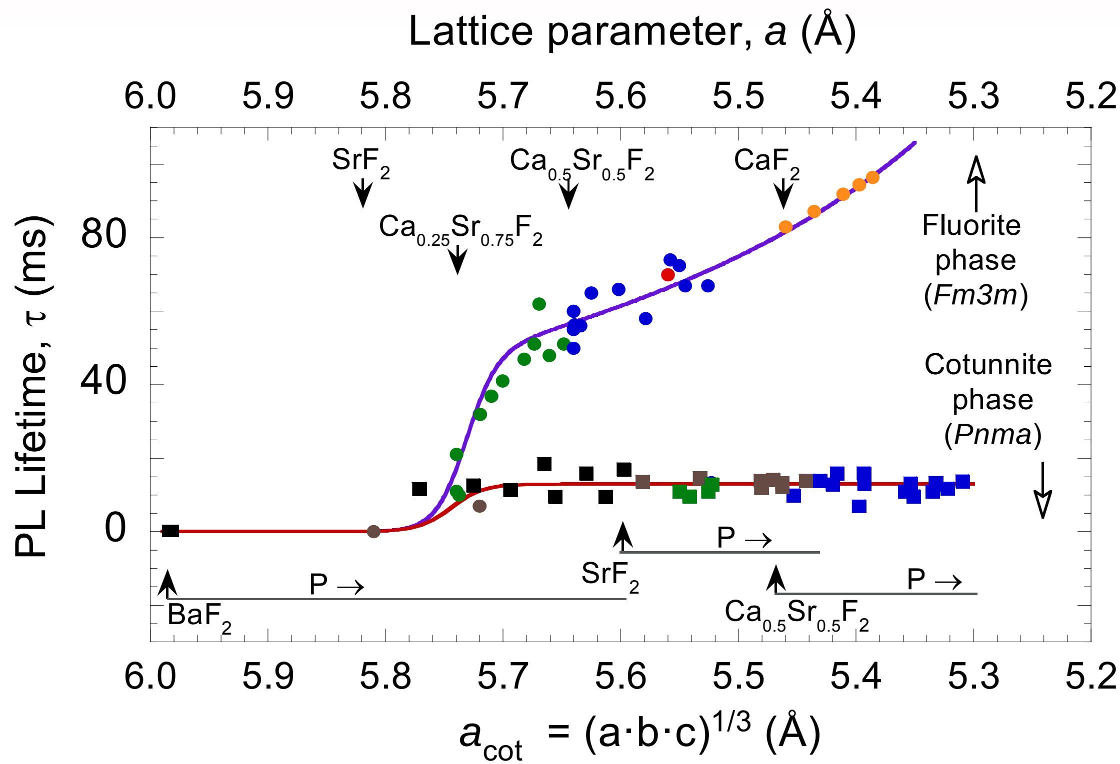

General behaviour.

Results - Fluorites

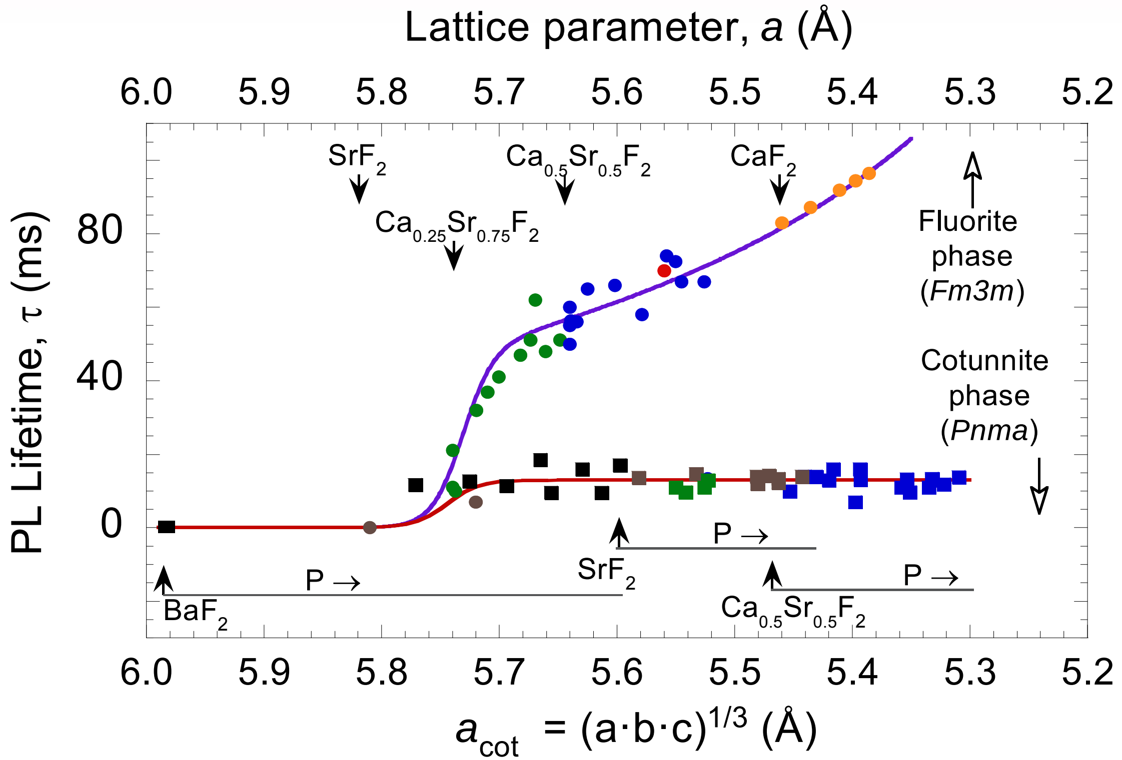

$$\tau^{-1}(a,T) = \underbrace{\tau_0^{-1} + \tau_{ED}^{-1}(a)\cdot \mathrm{Coth}\frac{\hbar\omega_u(a)}{2k_B T}}_{\tau_{rad}^{-1}(a,\,T)} + \underbrace{p(a)\cdot e^{-\frac{E_a(a)}{k_B T}}}_{\tau_{nr}^{-1}(a,\,T)}$$

General behaviour.

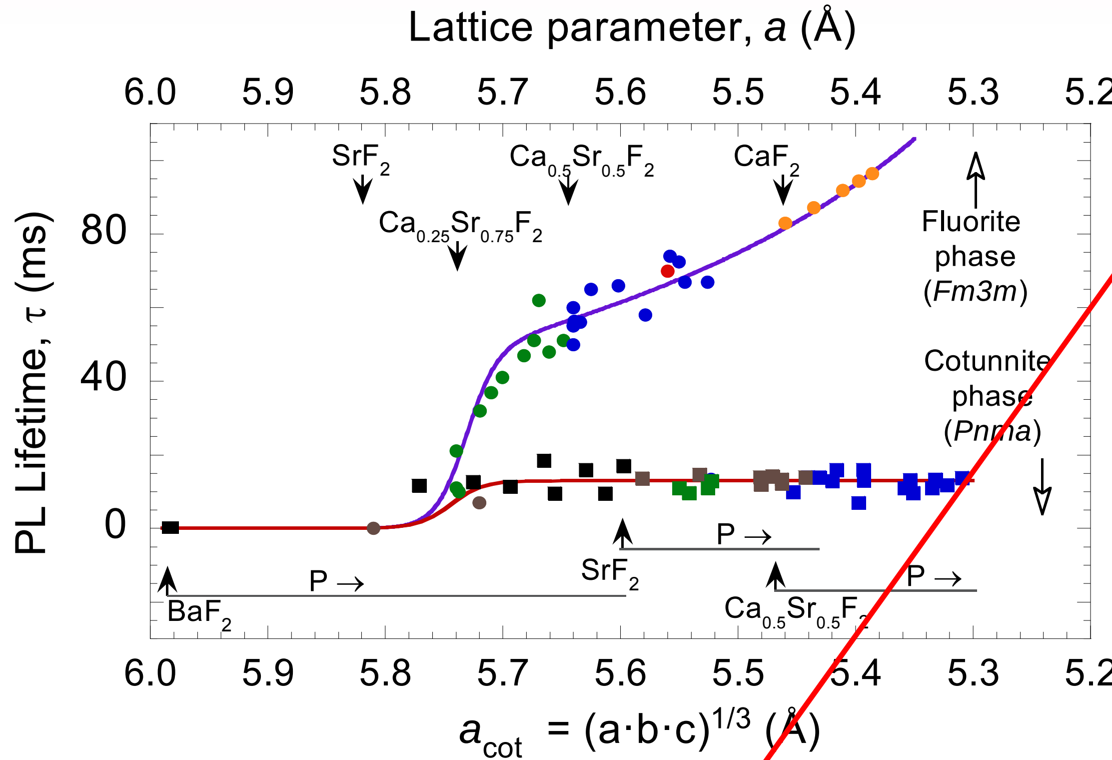

Phase-dependent geometry information

$$\tau^{-1}(a,T) = \underbrace{\tau_0^{-1} + \tau_{ED}^{-1}(a)\cdot \mathrm{Coth}\frac{\hbar\omega_u(a)}{2k_BT}}_{\tau_{rad}^{-1}(a,\ T)} + \underbrace{p(a)\cdot e^{-\frac{E_a(a)}{k_BT}}}_{\tau_{nr}^{-1}(a,\ T)}$$

General behaviour.

Results - Fluorites

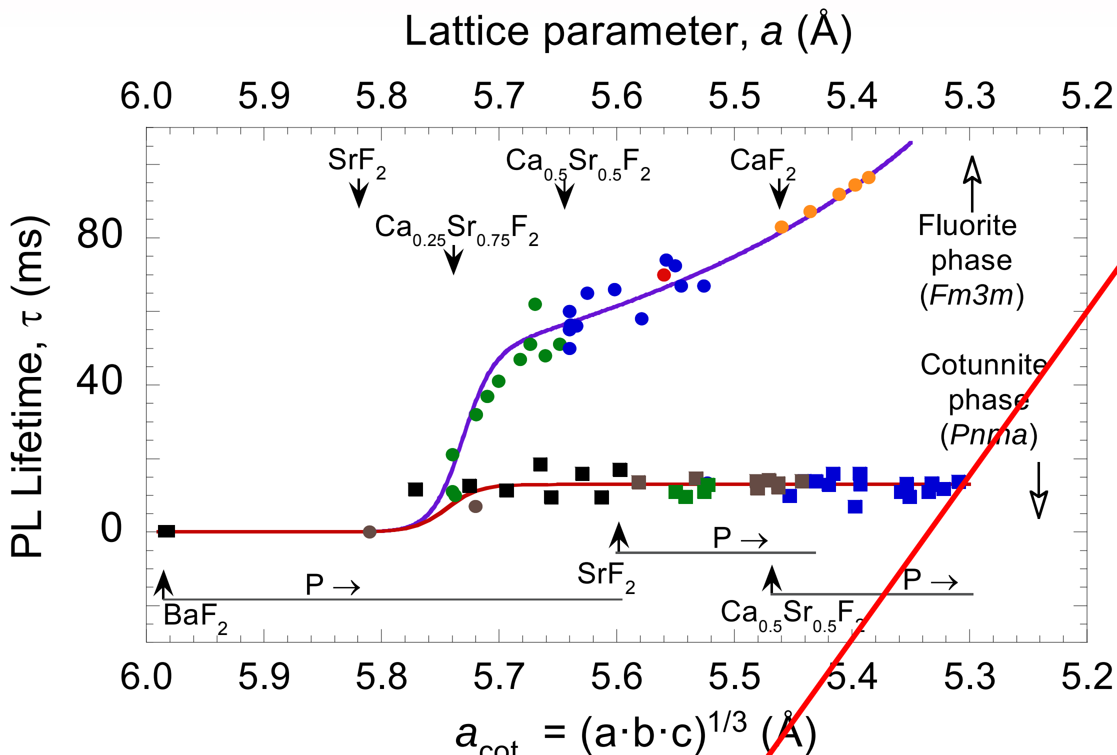

Phase-dependent geometry information

Phase-independent

$$\tau^{-1}(a,T) = \tau_0^{-1} + \tau_{ED}^{-1}(a)\cdot \mathrm{Coth}\frac{\hbar\omega_u(a)}{2k_B T} + p(a)\cdot e^{-\frac{E_a(a)}{k_B T}}$$

$\tau_{rad}^{-1}(a, T)$ $\quad$ $\tau_{nr}^{-1}(a, T)$

General behaviour.

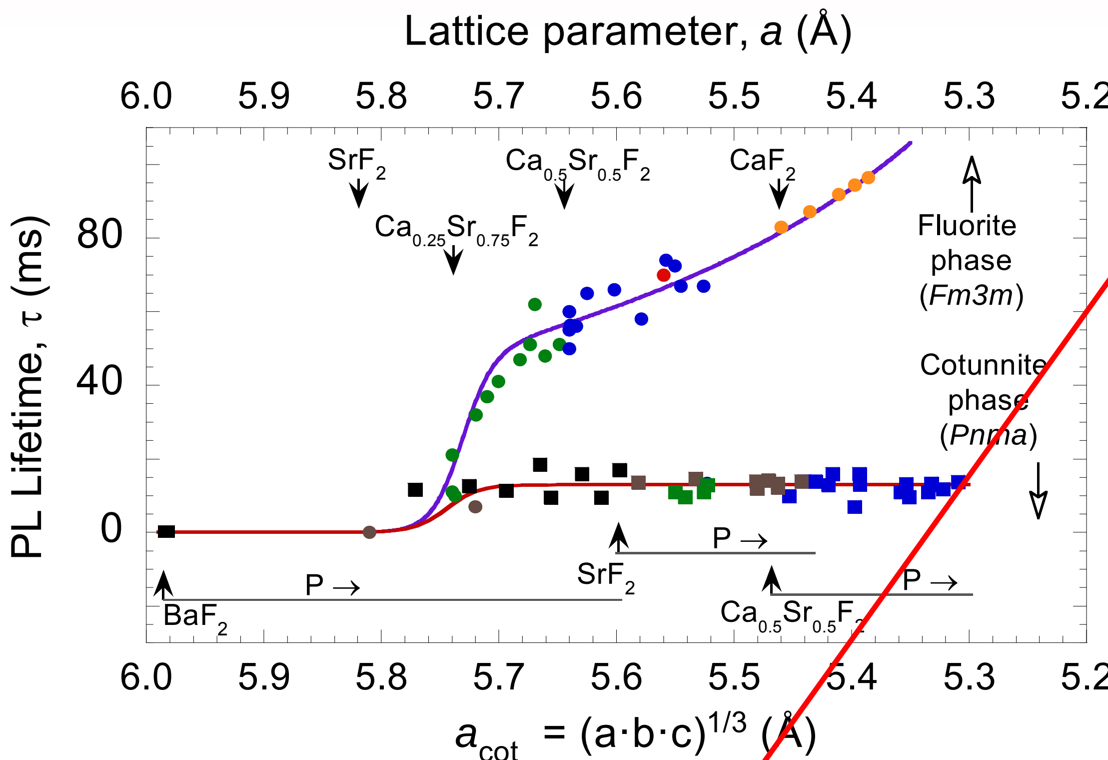

Phase-dependent geometry information

Phase-independent

$$\tau^{-1}(a,T) = \tau_0^{-1} + \tau_{ED}^{-1}(a)\cdot \mathrm{Coth}\frac{\hbar\omega_u(a)}{2k_BT} + p(a)\cdot e^{-\frac{E_a(a)}{k_BT}}$$

$\tau_{rad}^{-1}(a, T)$ $\tau_{nr}^{-1}(a, T)$

$v < 29\ cm^3/mol$

⇓

Photoluminescence

A_2BMF_6: Cr^{3+} Fluoroelpasolites

Optical spectra and structure correlations

Elpasolite structure.

A_2BMF_6: Cr^{3+}

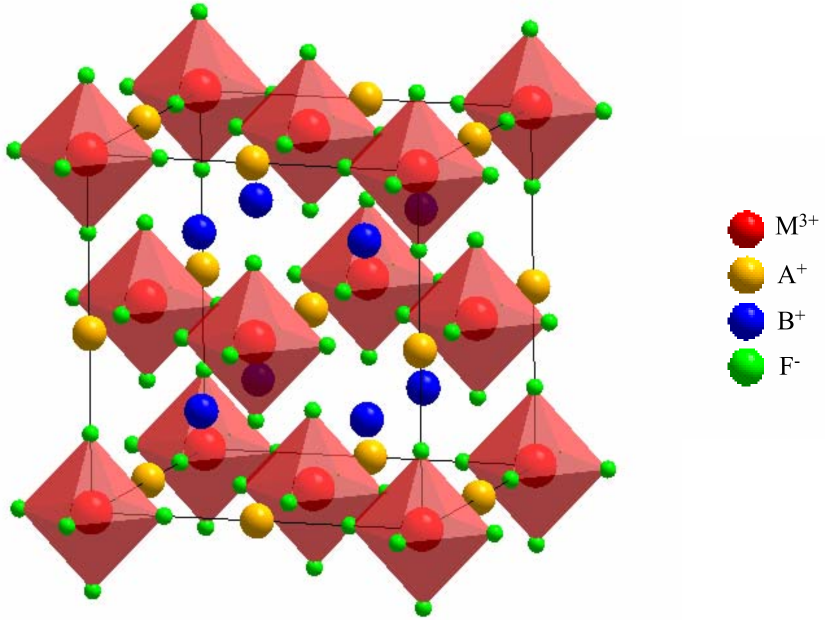

Elpasolite structure.

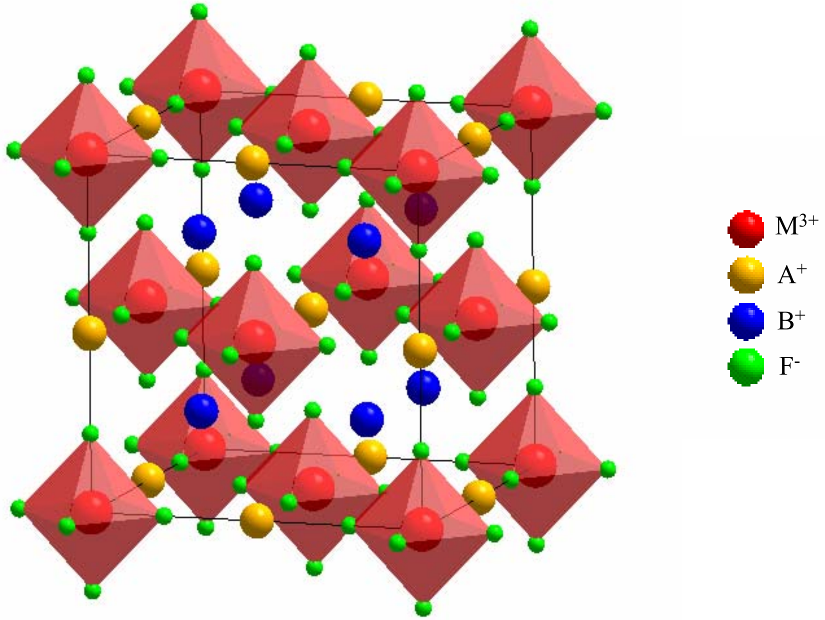

A_2BMF_6: Cr^{3+}

Independent octahedra

Parameters: a, x_F

$R_{M\text{-}F} = x_F \cdot a$

Elpasolite structure.

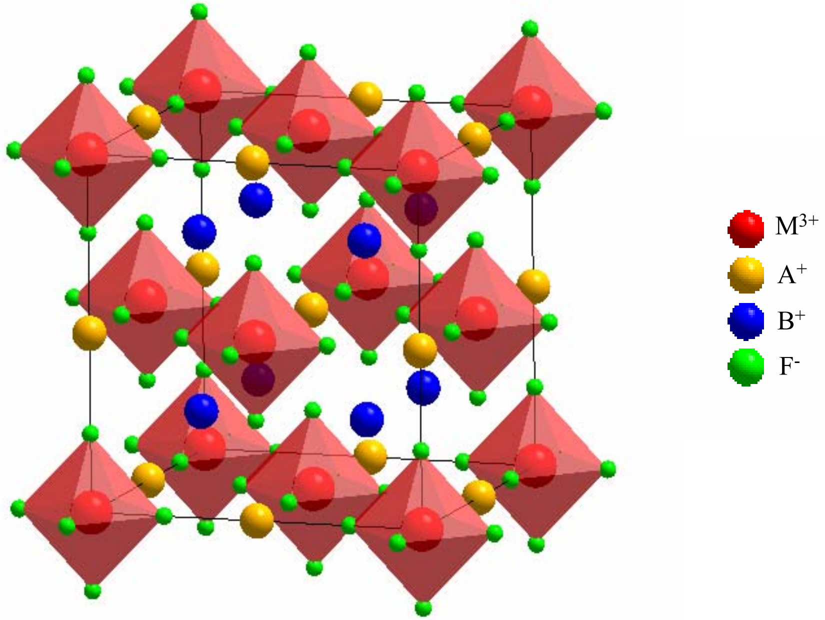

A_2BMF_6: Cr^{3+}

Independent octahedra

Parameters: a, x_F

$R_{M\text{-}F} = x_F \cdot a$

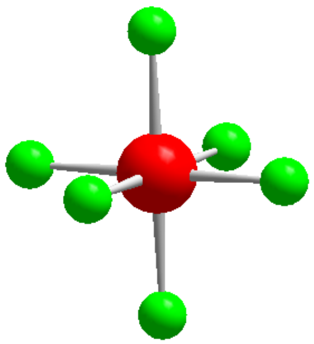

Simple structure around Cr^{3+} provides an interesting set of systems in order to establish opto-structural correlations

Electronic structure.

Cr^{3+}: d^3

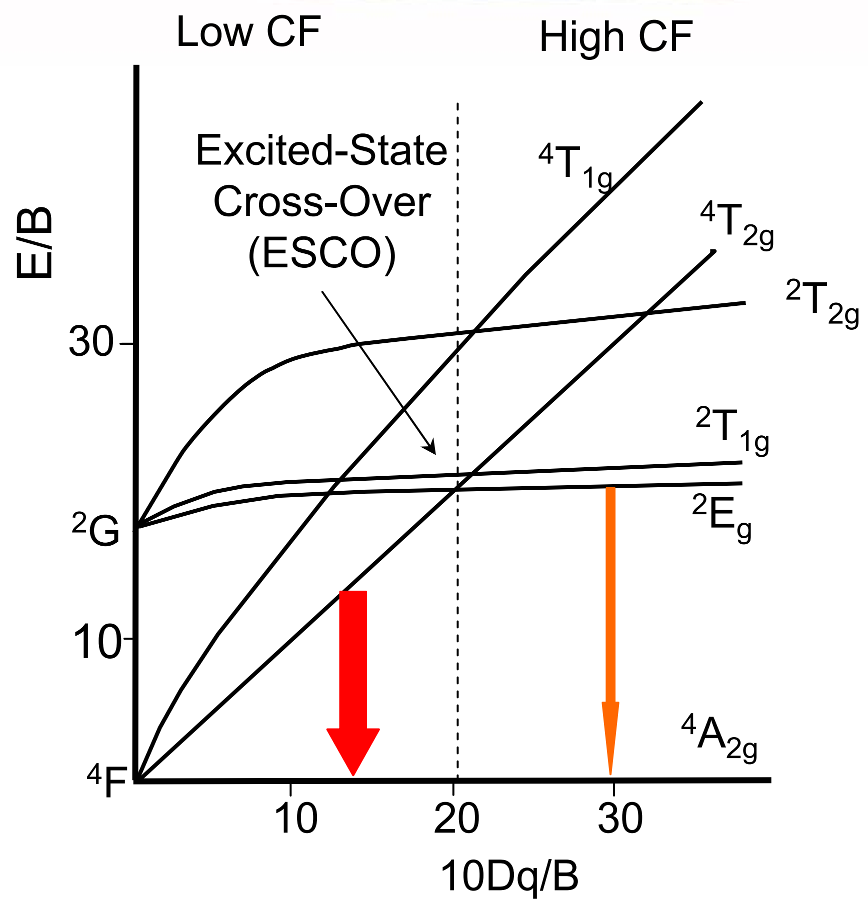

Broad-band

fast emission

Narrow lines (ruby-like)

slow emission

Spectroscopic results.

Results - Elpasolites

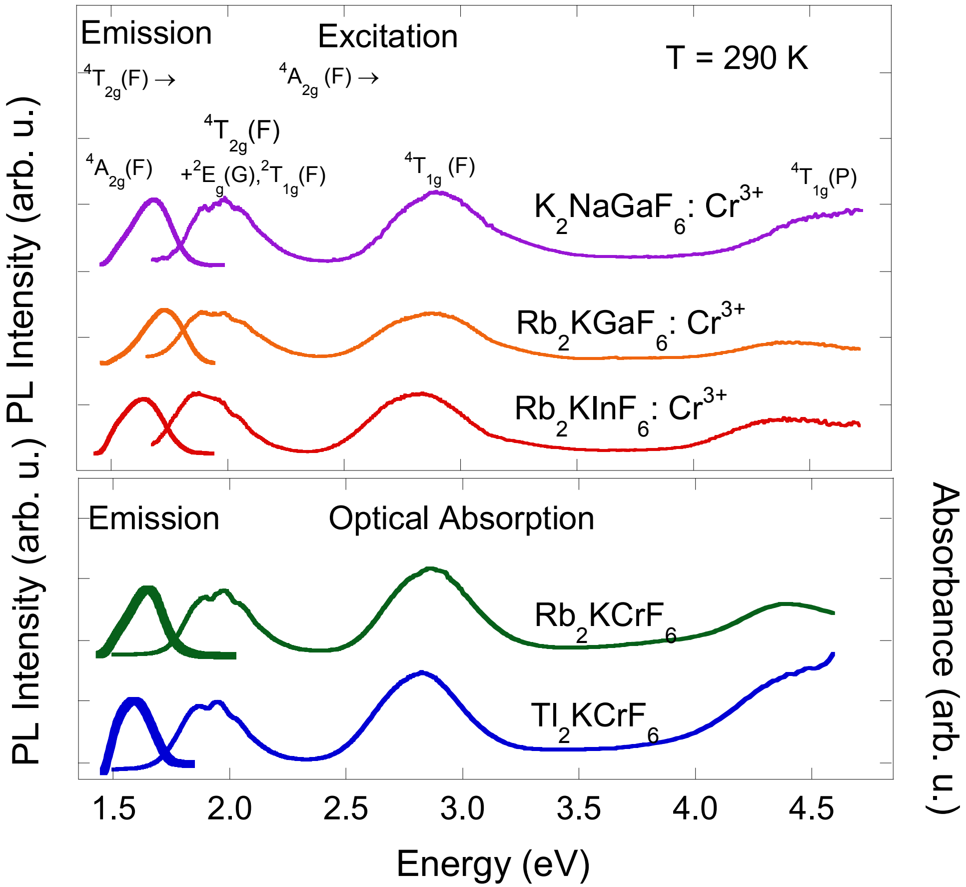

Spectroscopic results.

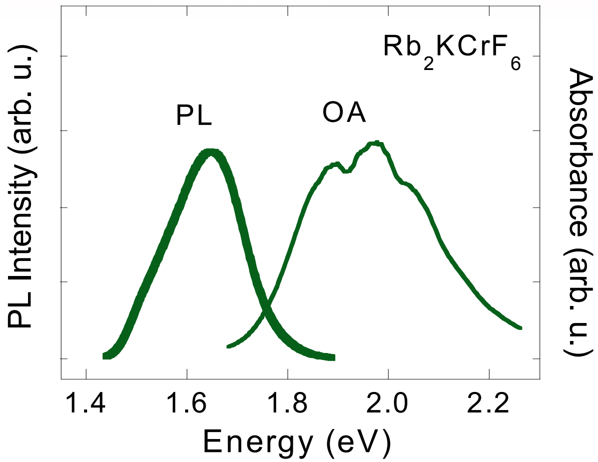

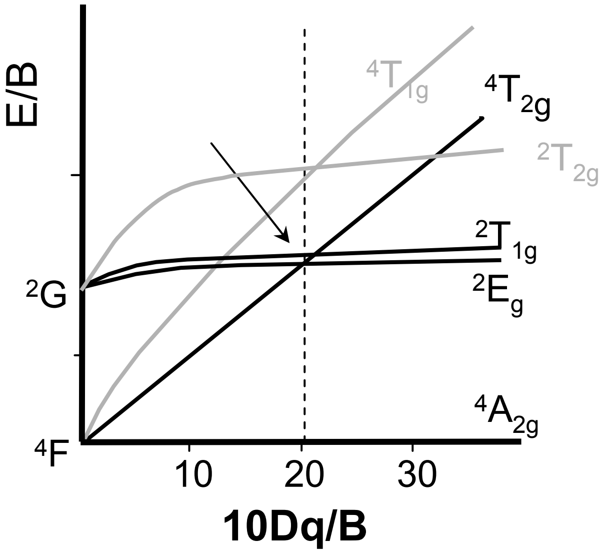

States anti-resonance
Close to ESCO

Results - Elpasolites

Spectroscopic results.

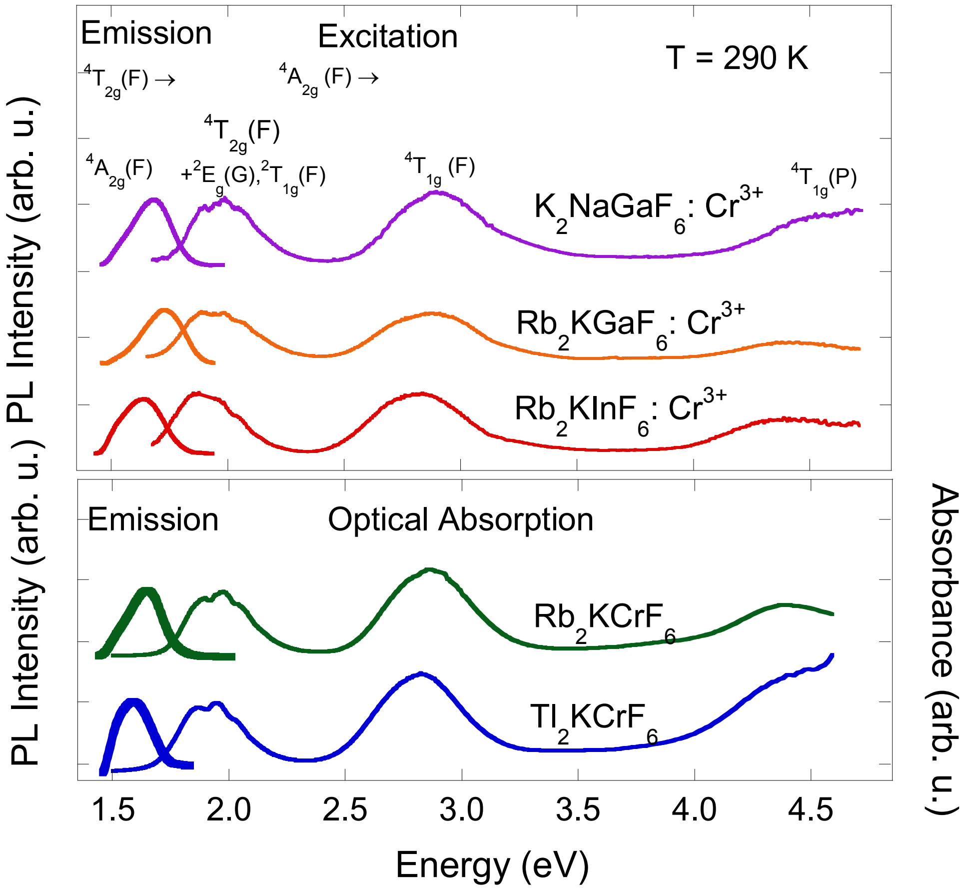

States anti-resonance
Close to ESCO

$\Delta 10Dq/10Dq \sim 3\%$

From Rb_2KInF_6: Cr^{3+}
(a = 9.098 Å)

to K_2NaGaF_6:Cr^{3+}
(a = 8.255 Å).

Structural characterization: XRD.

Pure compounds of the series → $R_{Cr\text{-}F}$

Structural characterization: XRD.

Pure compounds of the series → $R_{Cr\text{-}F}$

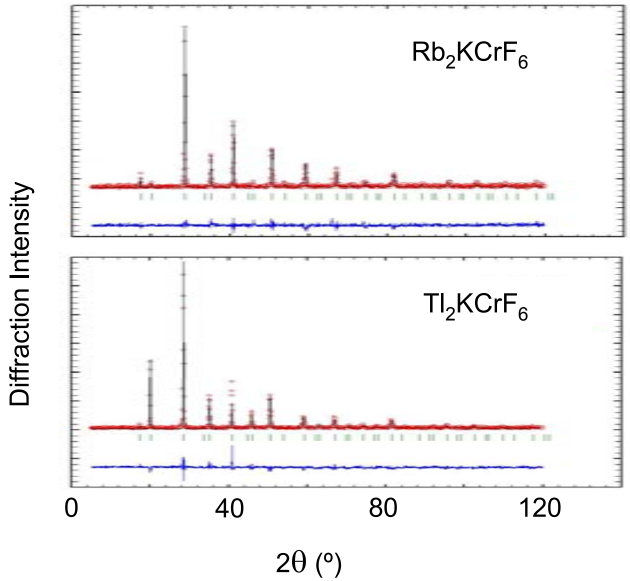

Powder XRD ⇒ low precission in x_F

Papers also report different x_F values.

Single crystal XRD: Massa, Rev. Ch. Min., **23**, 508 (1986)

	$R_{Cr\text{-}F}$ (Å) XRD
K_2NaCrF_6	1.897 ± 0.001
Rb_2KCrF_6	1.89 ± 0.01
Tl_2KCrF_6	1.93 ± 0.01

Structural characterization: Raman.

Pure compounds of the series → $R_{Cr\text{-}F}$

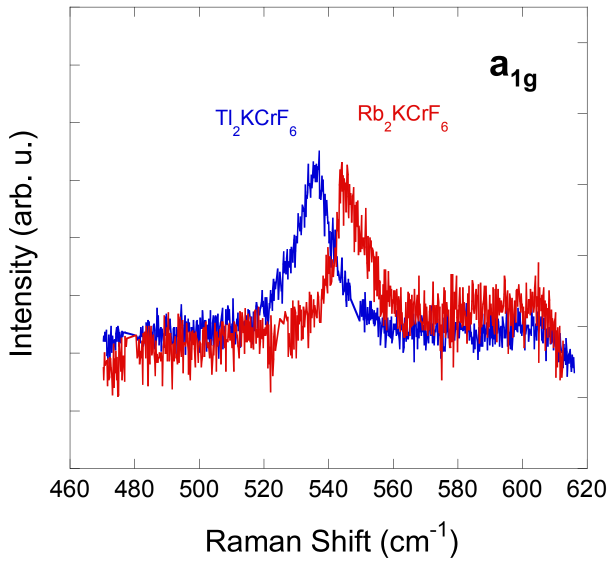

Local Grüneisen parameter:

$$\gamma_{a_{1g},local} = -\frac{\partial \ln \omega_{a_{1g}}}{\partial \ln V_{CrF_3^{3-}}} = -\frac{1}{3}\frac{\partial \ln \omega_{a_{1g}}}{\partial \ln R_{Cr-F}}$$

Woods et *al.* J.Phys. Chem. Sol. **54**, 543 (1993)

$$\hbar\omega_{a_{1g}} = \hbar K R_{Cr-F}^{-3\gamma_{a_{1g},local}}$$

		$R_{Cr\text{-}F}$ (Å)
	(cm^{-1})	XRD
K_2NaCrF_6	570 ± 2	1.897 ± 0.001
Rb_2KCrF_6	545 ± 2	1.89 ± 0.01
Tl_2KCrF_6	536 ± 2	1.93 ± 0.01

Structural characterization: Raman.

Pure compounds of the series → $R_{Cr\text{-}F}$

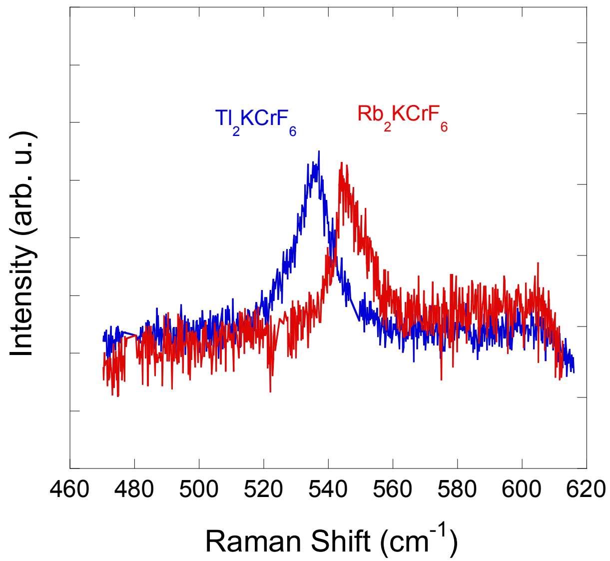

Local Grüneisen parameter:

$$\gamma_{a_{1g},local} = -\frac{\partial \ln \omega_{a_{1g}}}{\partial \ln V_{CrF_3{}^{3-}}} = -\frac{1}{3}\frac{\partial \ln \omega_{a_{1g}}}{\partial \ln R_{Cr-F}}$$

Woods et *al.* J.Phys. Chem. Sol. **54**, 543 (1993)

$$\hbar\omega_{a_{1g}} = \hbar K R_{Cr-F}{}^{-3\gamma_{a_{1g},local}}$$

Reference

K_2NaCrF_6

		$R_{Cr\text{-}F}$ (Å)	
	(cm^{-1})	a_{1g}	XRD
K_2NaCrF_6	570±2	1.897 ± 0.001	1.897 ± 0.001
Rb_2KCrF_6	545±2	1.911 ± 0.005	1.89 ± 0.01
Tl_2KCrF_6	536±2	1.920 ± 0.005	1.93 ± 0.01

10Dq as a function of $R_{Cr\text{-}F}$.

10Dq vs. $R_{Cr\text{-}F}$ for A_2BCrF_6 (Cr^{3+}-pure compunds of the series)

10Dq as a function of $R_{Cr\text{-}F}$.

Results - Elpasolites

10Dq vs. $R_{Cr\text{-}F}$ for A_2BCrF_6 (Cr^{3+}-pure compunds of the series)

$$10Dq \propto R_{Cr\text{-}F}^{\ -n}$$

$10Dq \propto R_{Cr\text{-}F}^{-3.3}$ instead of $R_{Cr\text{-}F}^{-5}$ (calculated) for pure compunds

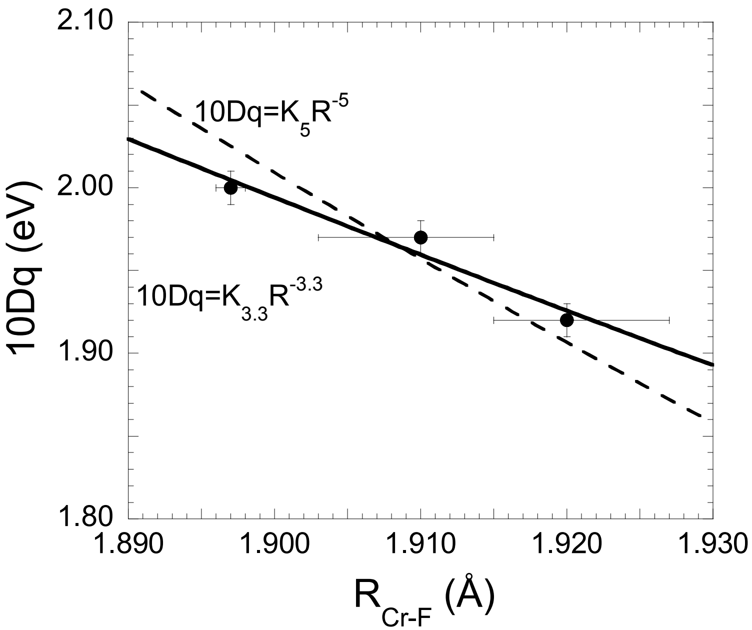

10Dq as a function of $R_{Cr\text{-}F}$.

10Dq vs. $R_{Cr\text{-}F}$ for A_2BCrF_6 (Cr^{3+}-pure compunds of the series)

$10Dq \propto R_{Cr\text{-}F}^{\ -n}$

$10Dq \propto R_{Cr\text{-}F}^{-3.3}$ instead of $R_{Cr\text{-}F}^{-5}$ (calculated) for pure compunds

We are measuring the 1st band, but it is a spin-orbit mixture of states.

Only one of them varies as 10Dq

$\Rightarrow \quad 5/3 < n < 5$

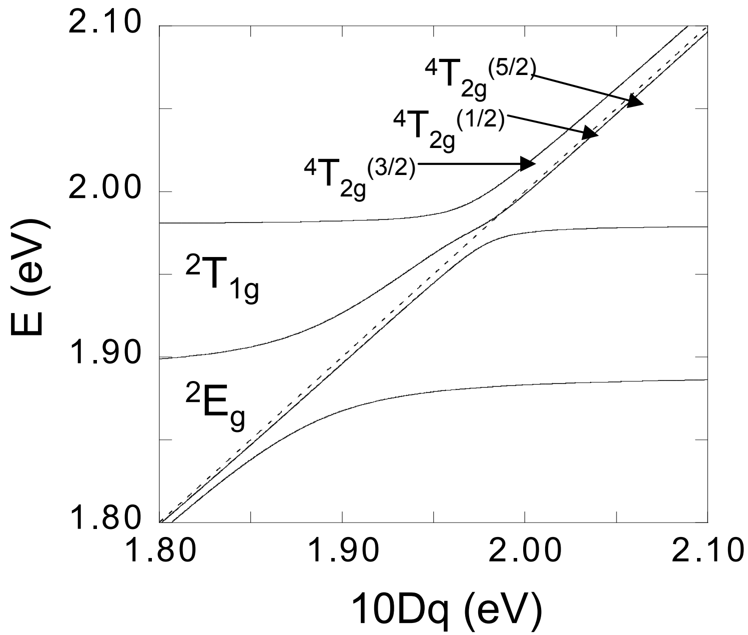

Structural correlations between *a*, $R_{M\text{-}F}$ and ΔE_{Stokes}.

Structural correlations between a, $R_{M\text{-}F}$ and ΔE_{Stokes}.

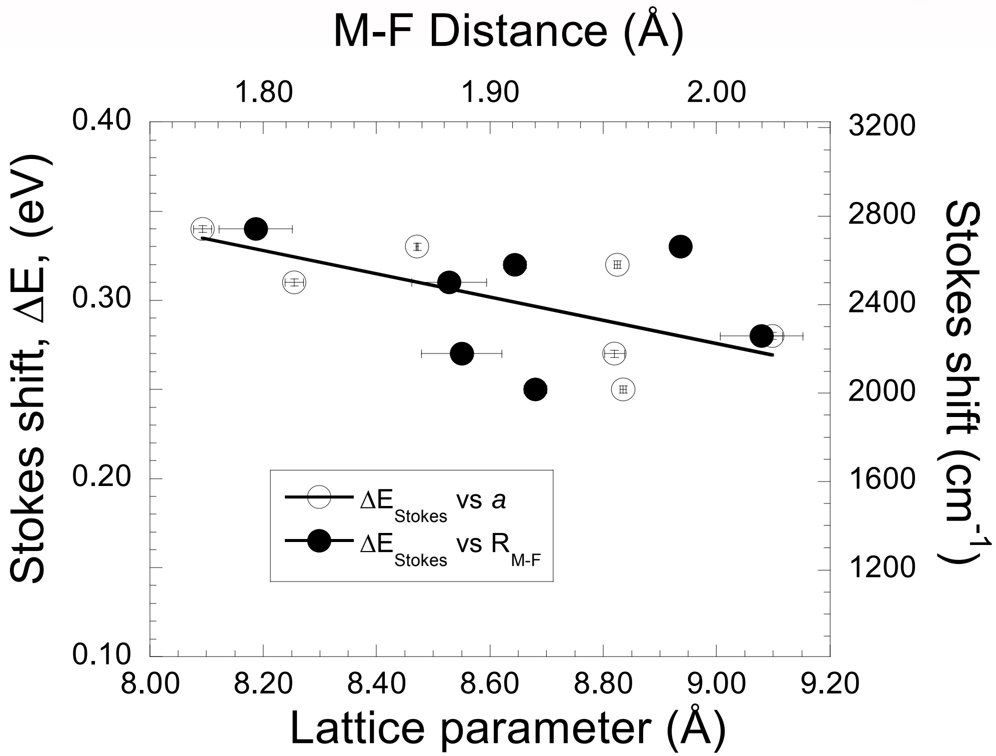

Highly scattered values

$R_{M\text{-}F} \downarrow \quad \Rightarrow \quad \Delta E_{Stokes} \uparrow$

(trend)

Results - Elpasolites

Structural correlations between *a*, R_{M-F} and ΔE_{Stokes}.

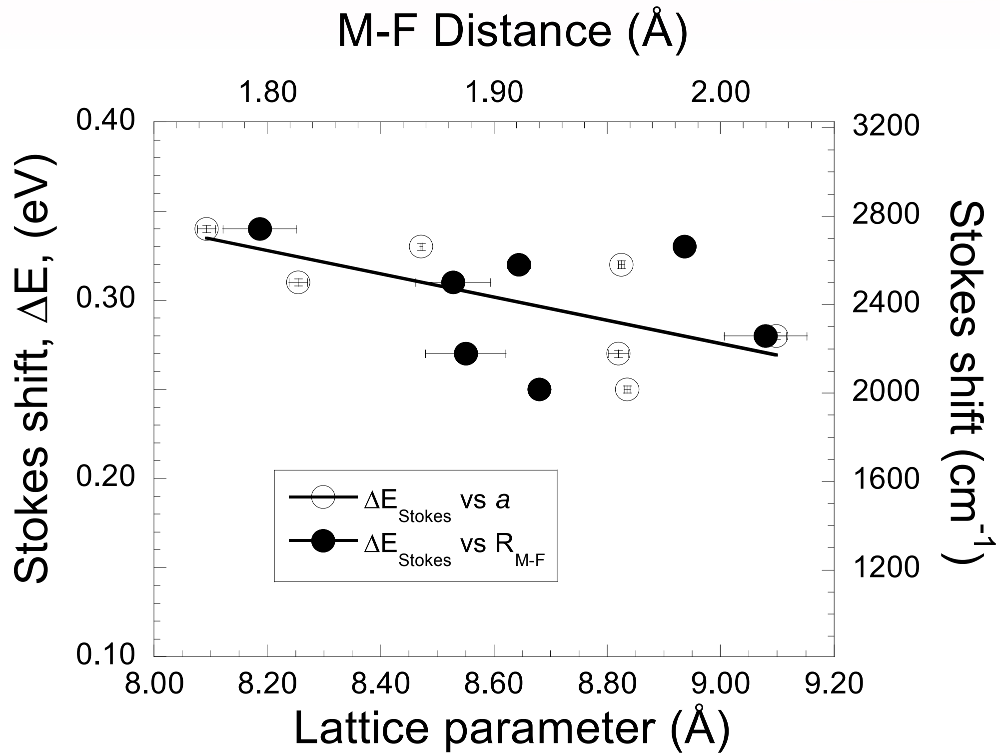

Highly scattered values

$R_{M-F} \downarrow \;\Rightarrow\; \Delta E_{Stokes} \uparrow$

(trend)

Local Cr-F distance governs optical properties

Pressure experiments. Stokes shift vs. P.

Pressure experiments. Stokes shift vs. P.

Rb_2KCrF_6

Emission + excitation

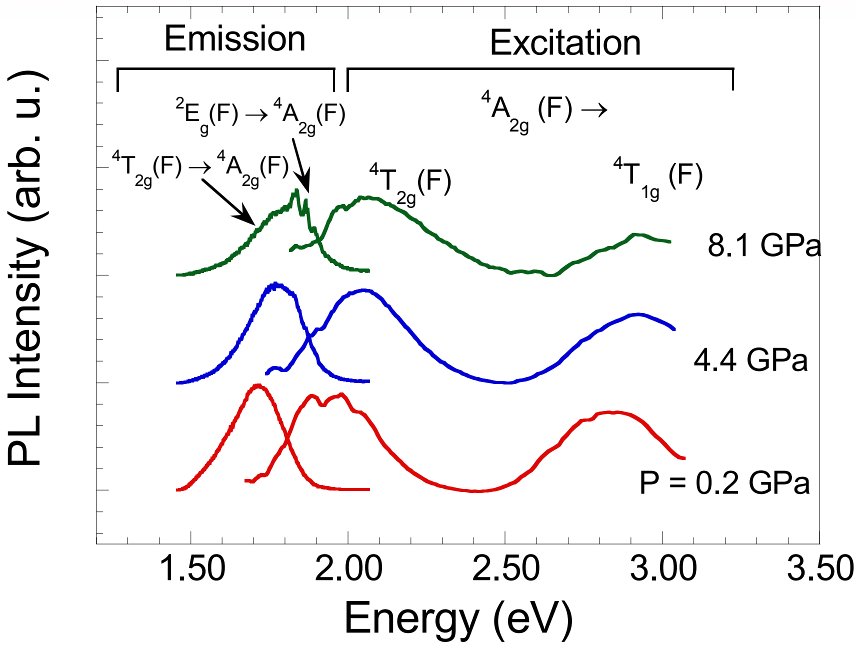

Pressure experiments. Stokes shift . P.

Results - Elpasolites

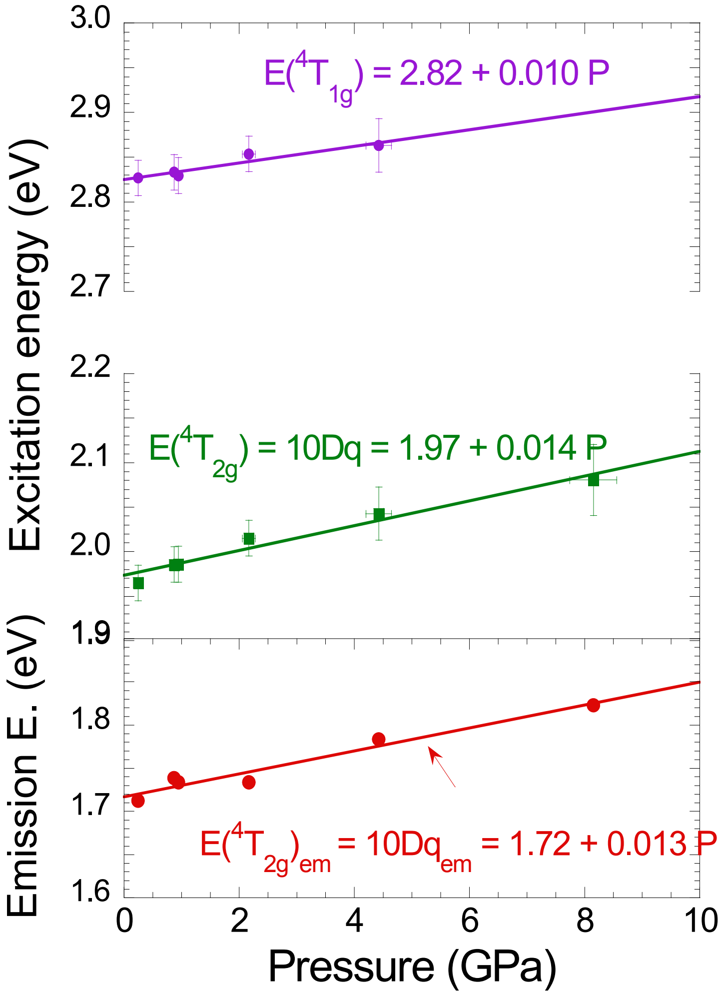

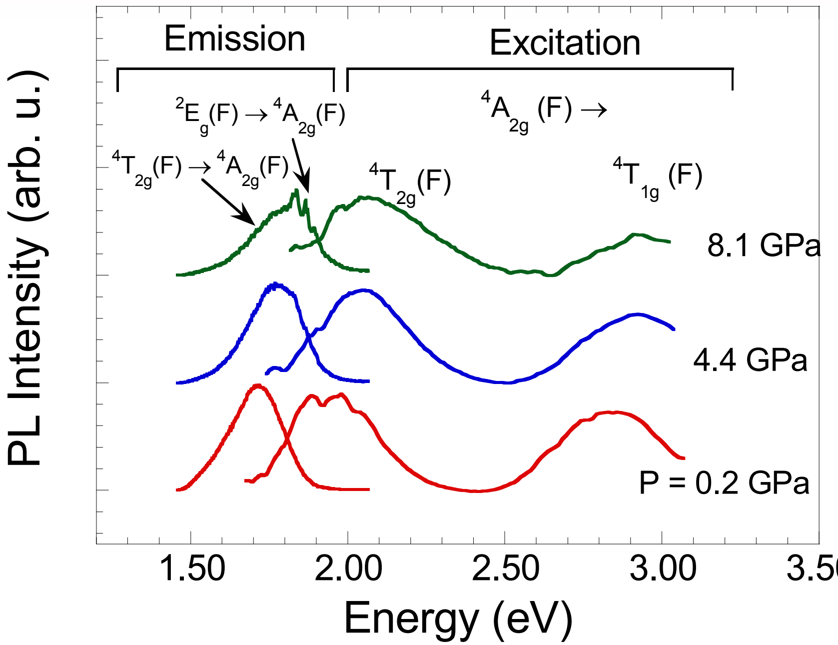

Pressure experiments. Stokes shift . P.

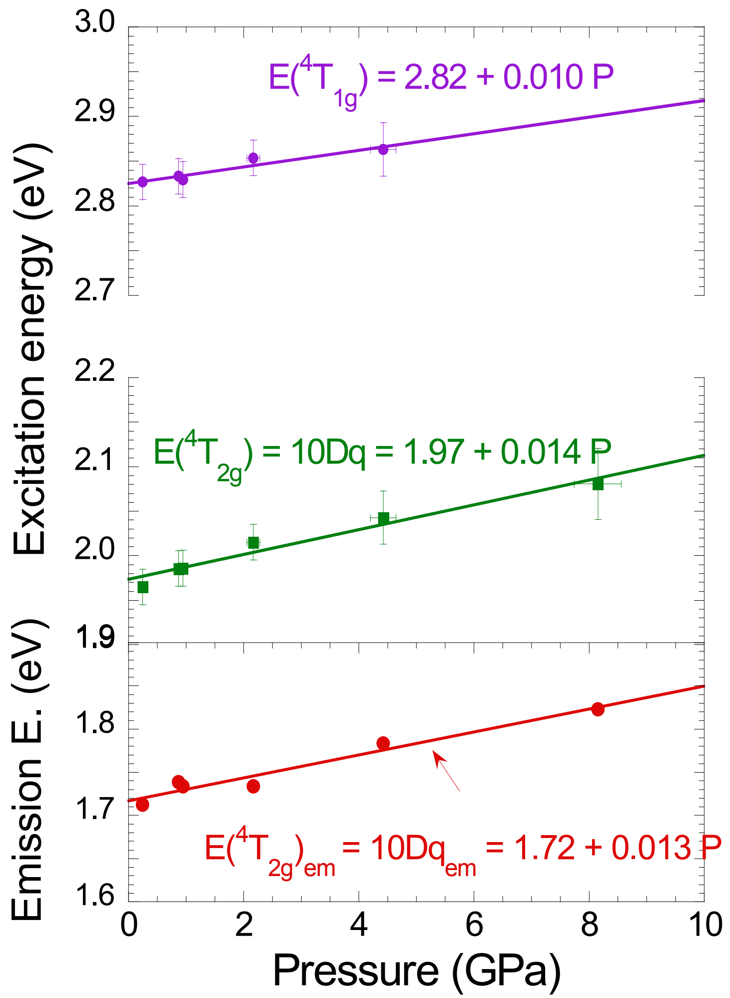

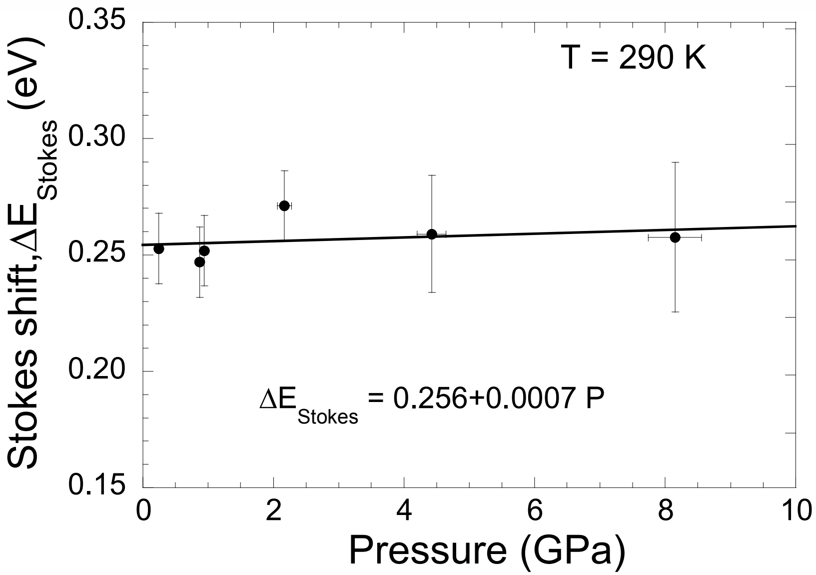

Stokes shift increases with P

Results - Elpasolites

Pressure experiments. Stokes shift . P.

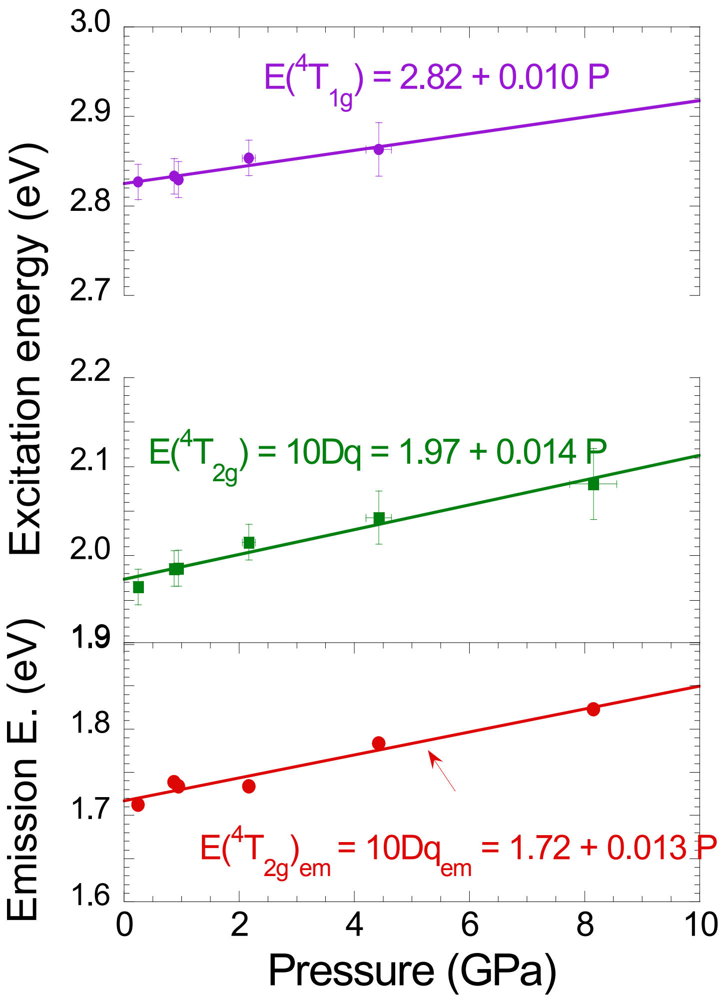

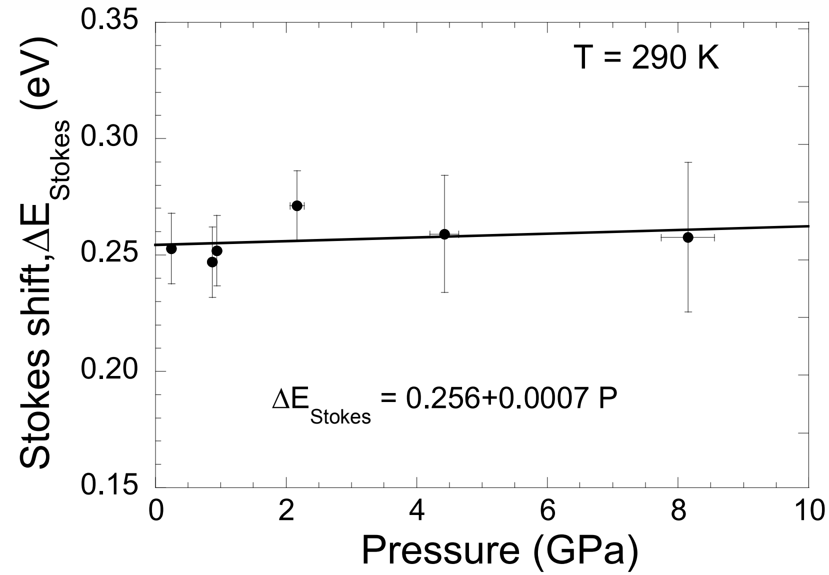

Stokes shift increases with P

Contrary to Cs_2NaMCl_6: Cr^{3+} and ABF_3: Mn^{2+}

Excited states proximity

Pressure experiments. Stokes shift . P.

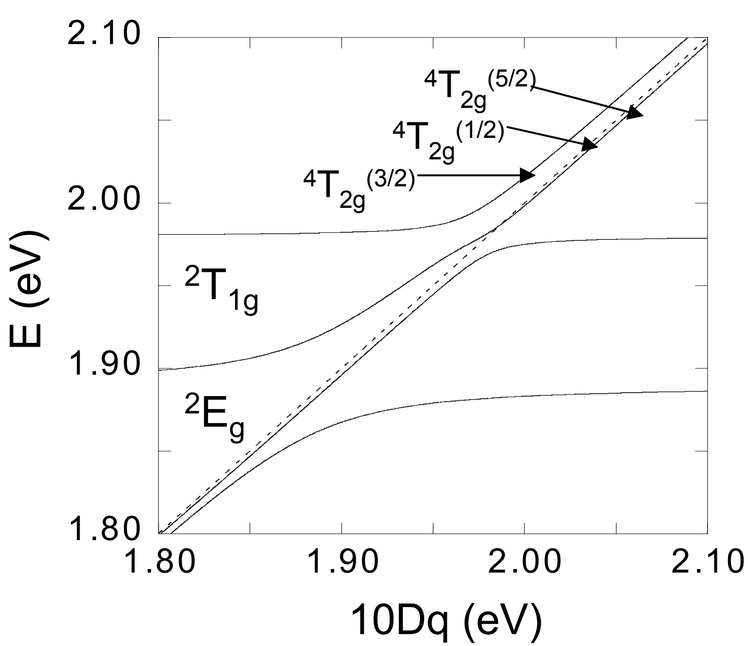

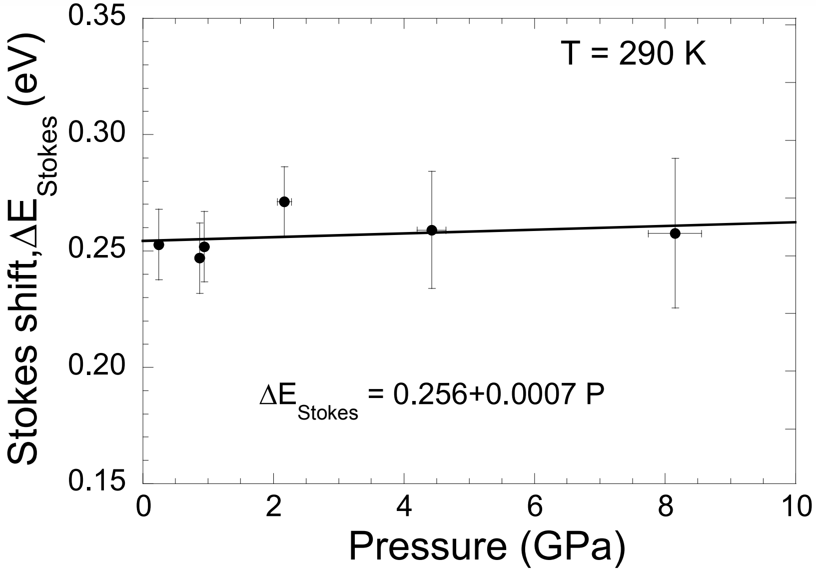

Stokes shift increases with P

Contrary to Cs_2NaMCl_6: Cr^{3+} and ABF_3: Mn^{2+}

Excited states proximity

Pressure-induced transformations in the spectrum: Excited State Crossover.

Rb_2KCrF_6

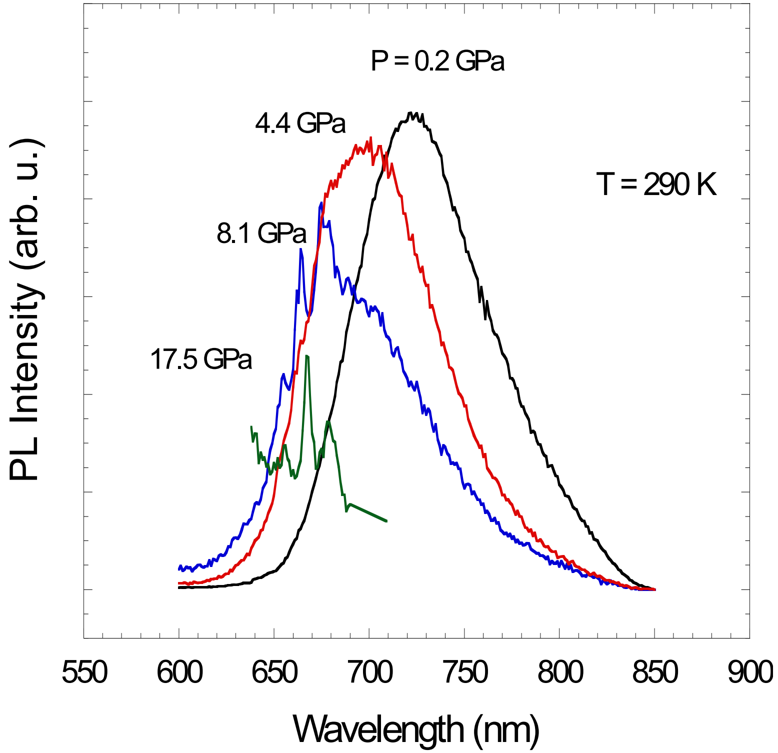

Band-shape transformation.
From broad band to narrow lines.

Excited State Crossover

Excited state crossover (ESCO).

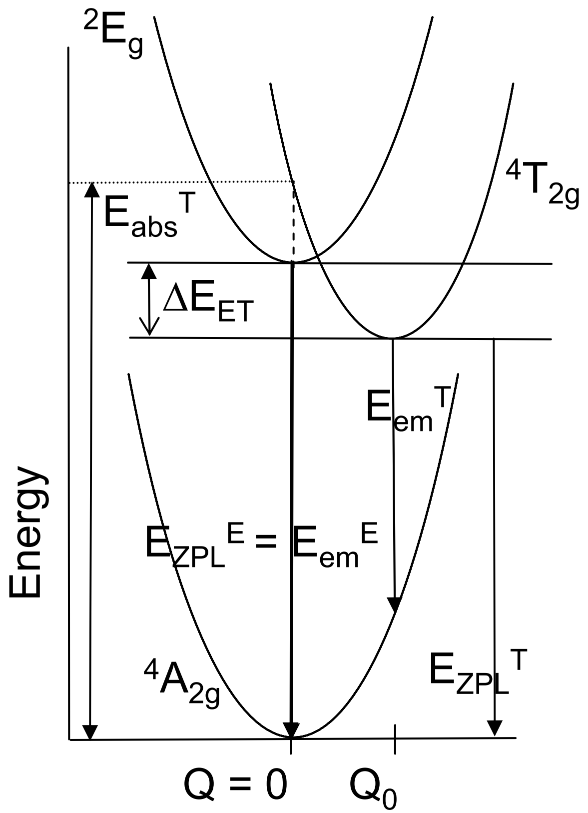

$E_{ZPL}^T < E_{ZPL}^E$

Excited state crossover (ESCO).

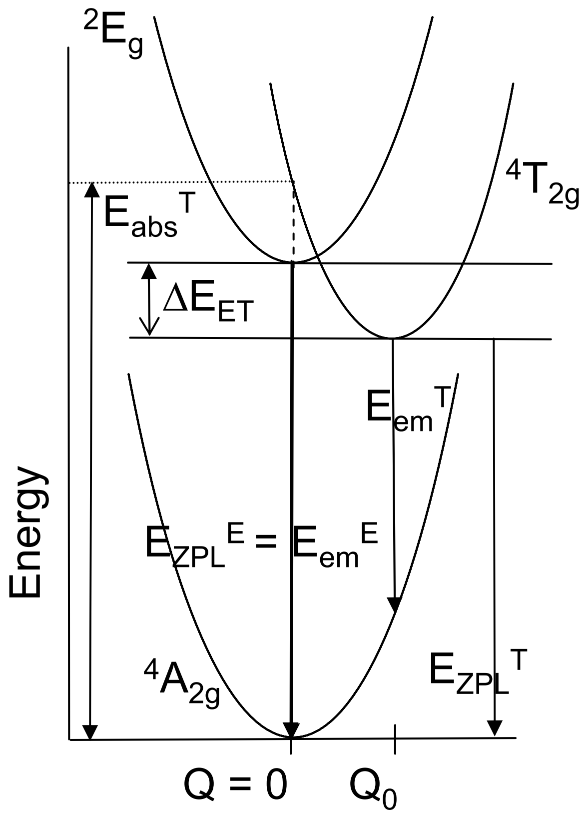

$E_{ZPL}^T < E_{ZPL}^E$

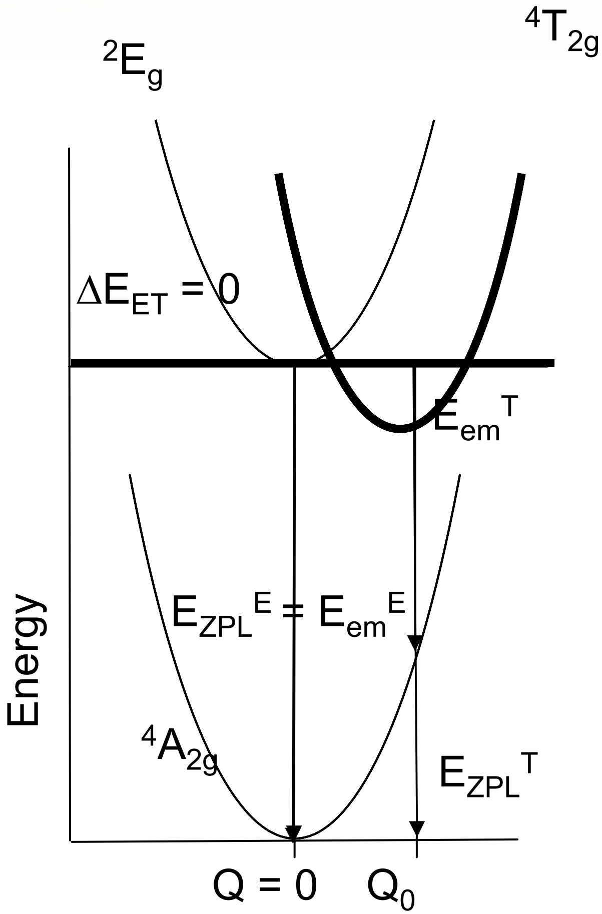

$E_{ZPL}^T = E_{ZPL}^E$

Excited state crossover (ESCO).

Results - Elpasolites

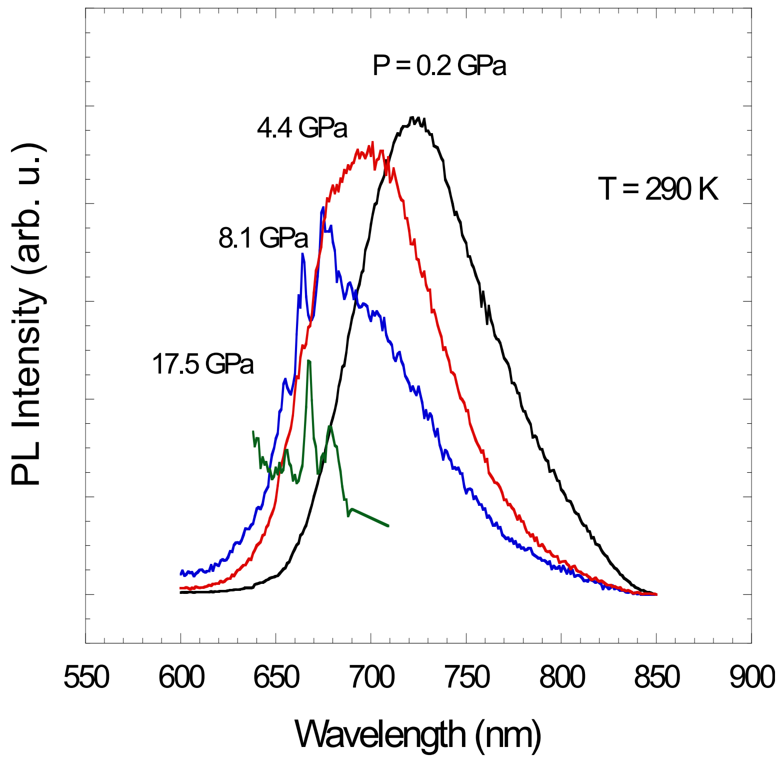

ESCO occurs before the dominance of narrow lines

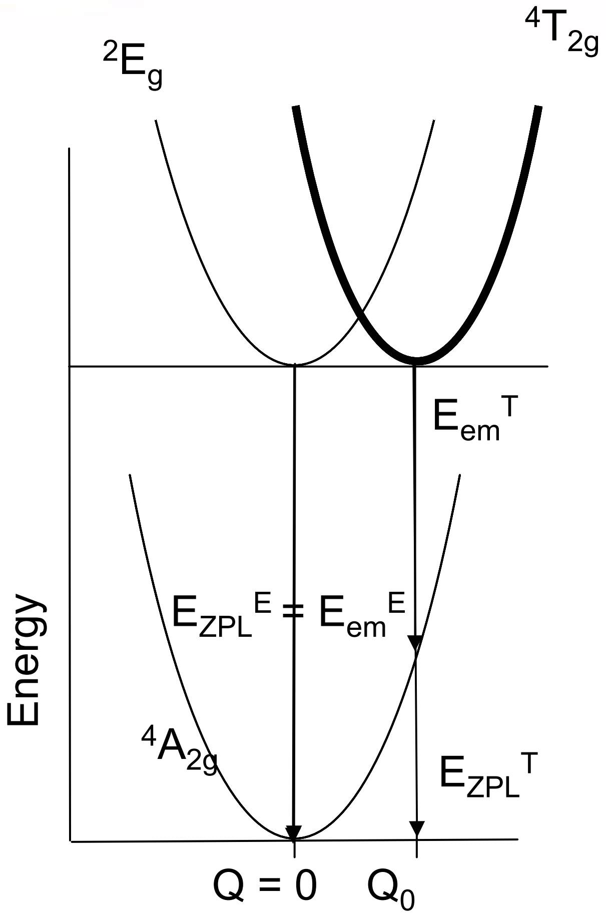

$E_{ZPL}^T > E_{ZPL}^E$

Excited state crossover (ESCO).

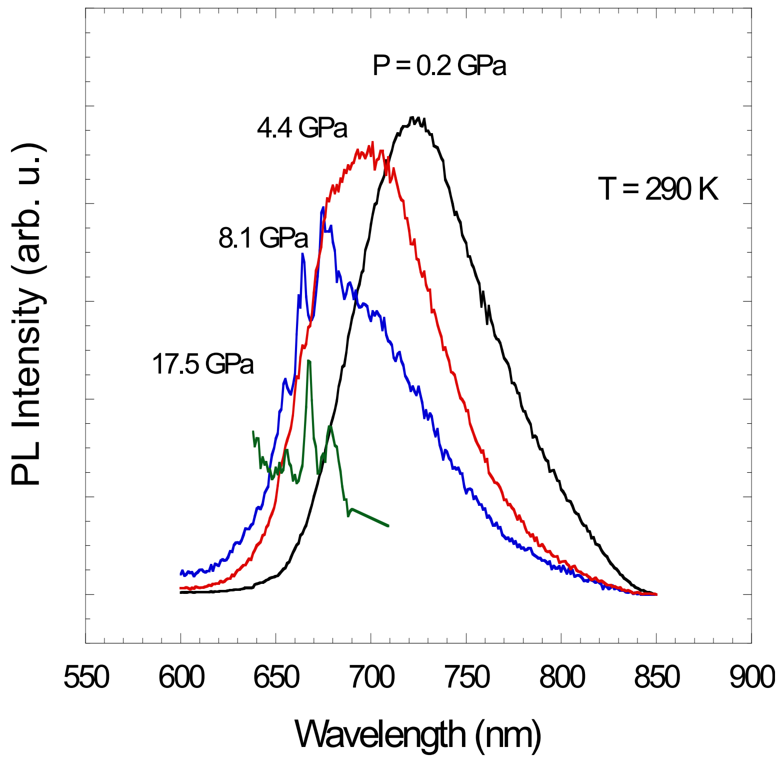

ESCO occurs before the dominance of narrow lines

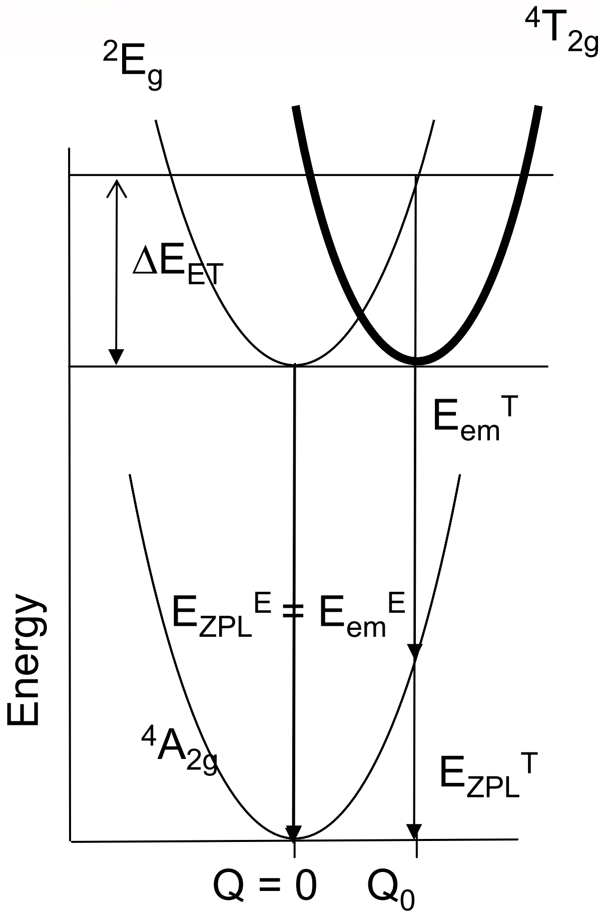

$E_{ZPL}{}^T > E_{ZPL}{}^E$

Changes in PL Lifetime.

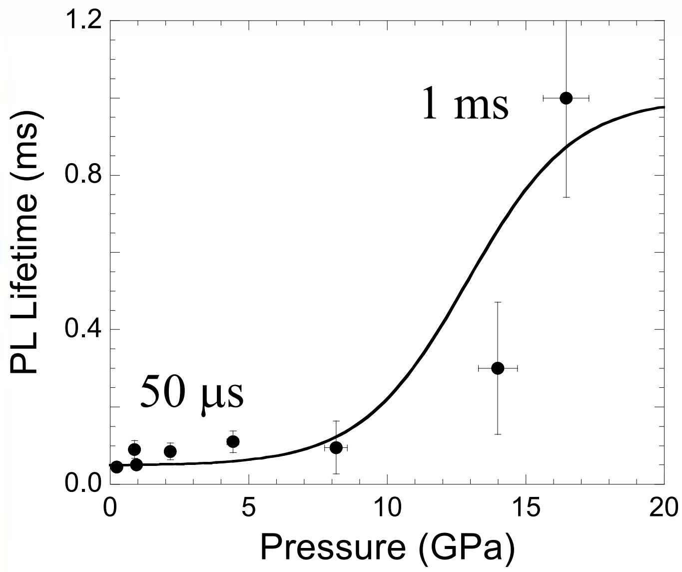

Changes in PL Lifetime.

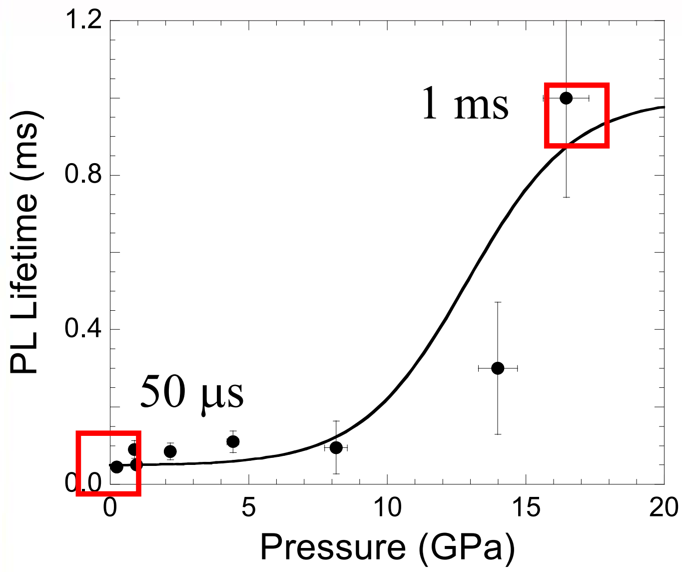

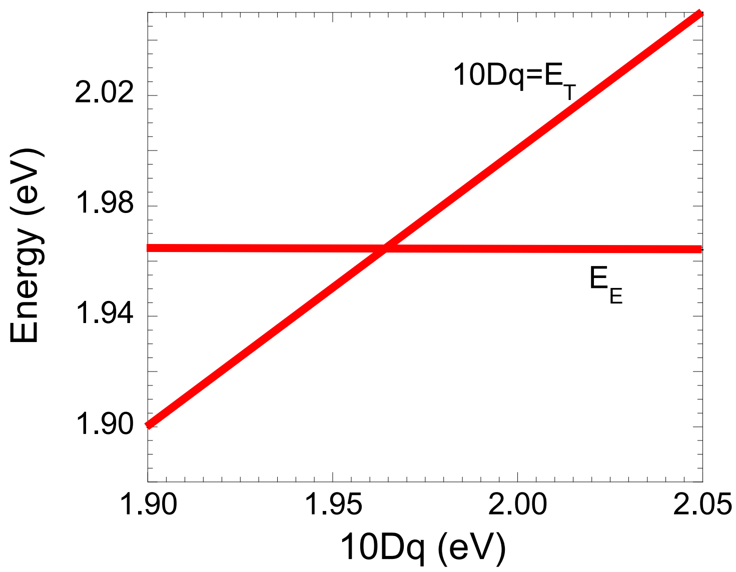

Changes in PL Lifetime.

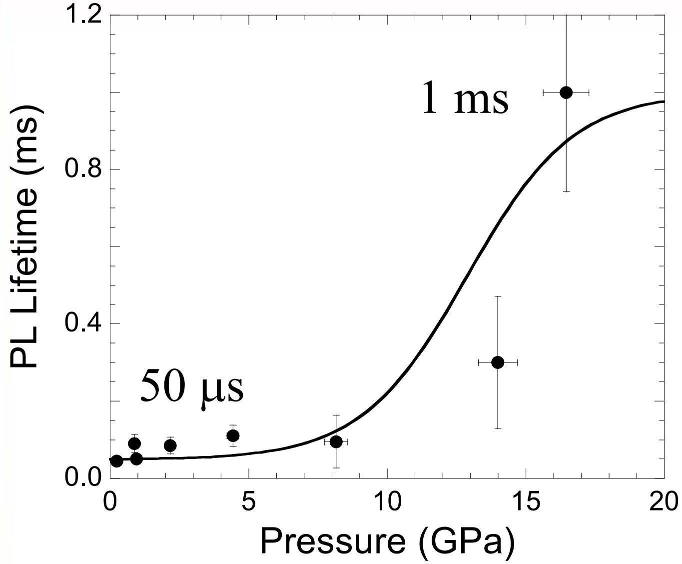

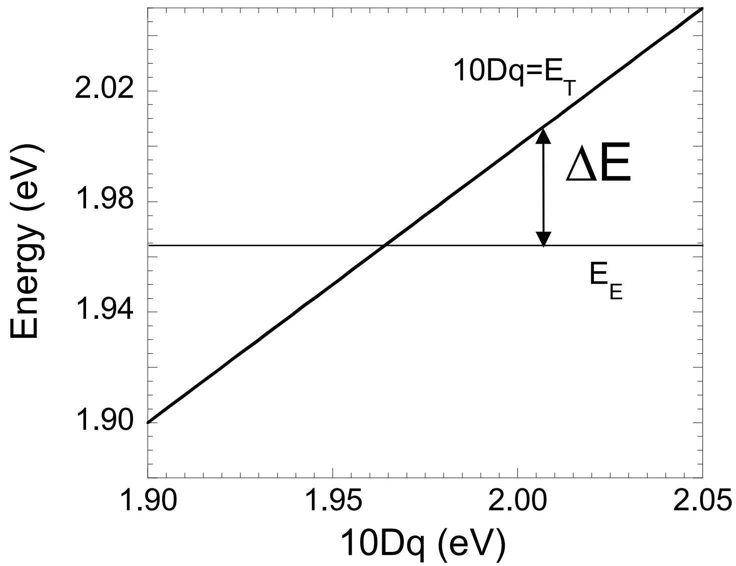

$$\tau^{-1}(P) = \frac{g_T \tau_T^{-1} e^{-\frac{\Delta E(P)}{k_B T}} + g_{ET}\tau_{ET}^{-1}}{g_T e^{-\frac{\Delta E(P)}{k_B T}} + g_{ET}}$$

$$\Delta E \uparrow \Rightarrow \tau^{-1} \downarrow$$

MnF_2

PL in concentrated transition metal ion systems

MnF_2 structure and energy states.

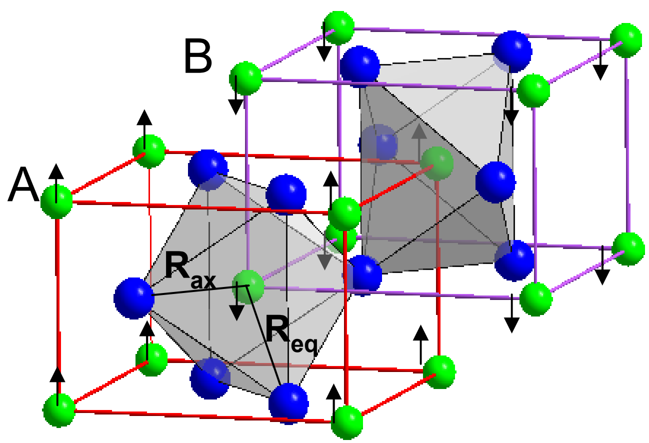

Quasi-octahedral coordination

Tanabe-Sugano Diagram

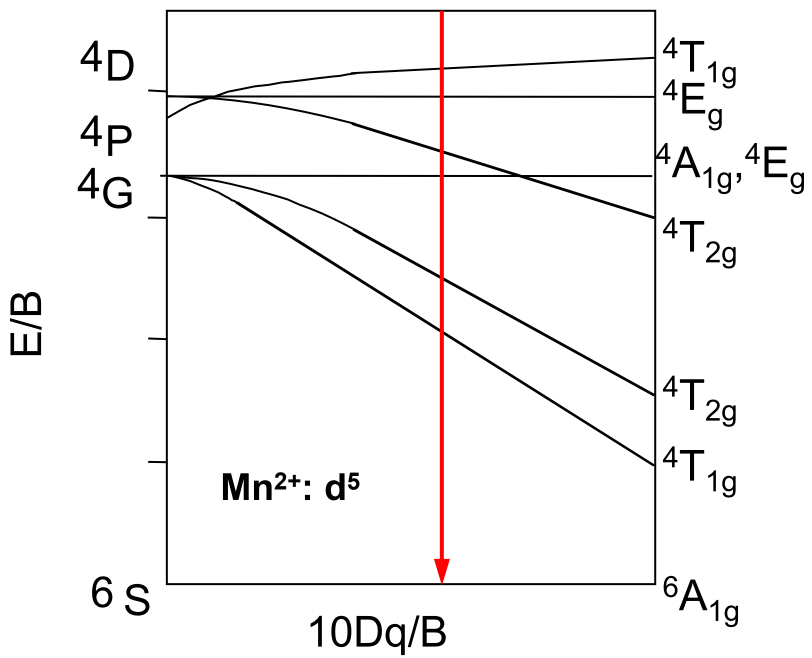

MnF_2 Luminescence at LT.

Results - MnF_2

MnF_2 Rutile

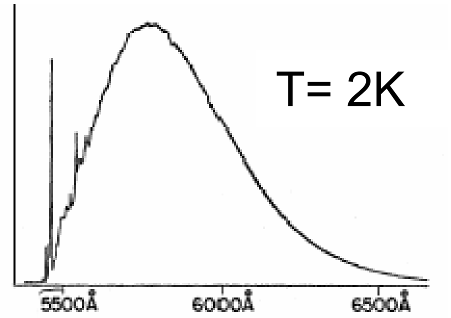

Greene et *al.* Phys Rev. **171**, 600 (1968)

v = 23.5 cm^3/mol

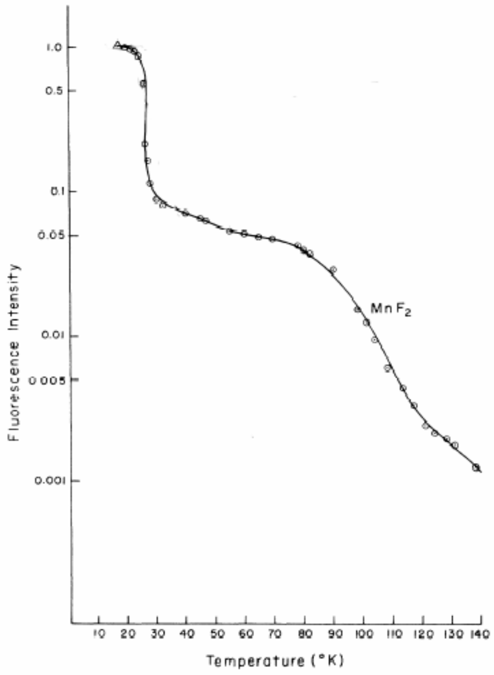

Holloway et *al.* Phys Rev. Lett **11**, 62 (1963)

PL Quenching for T > 140 K

↑

Excitation transfer to non-PL centers!

Excitons. PL traps in MnF_2.

Excitation migration and trapping

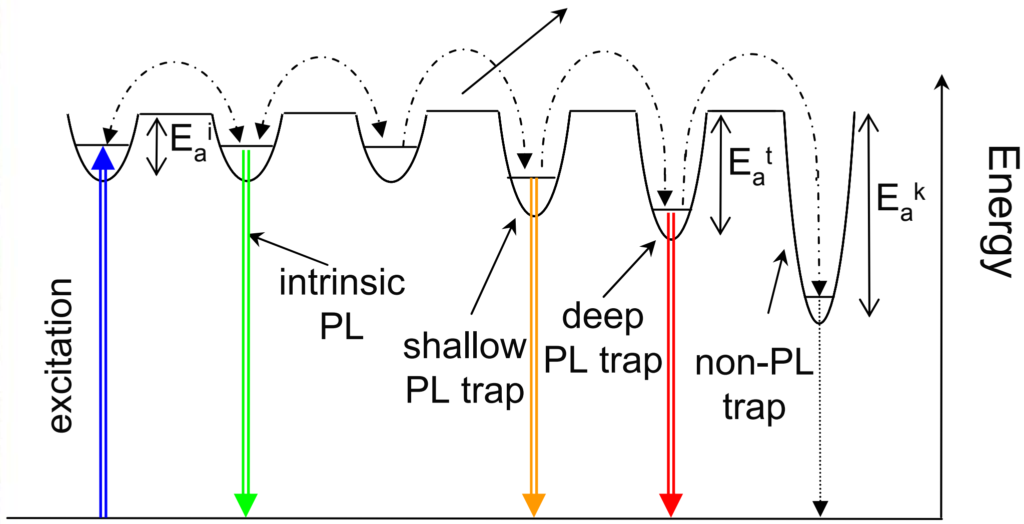

$$w_{DA} \propto |\langle \text{Donor},\text{Acceptor}^* \mid H_{int} \mid \text{Donor}^*,\text{Acceptor} \rangle|^2$$

Excitons. PL traps in MnF_2.

Excitation migration and trapping

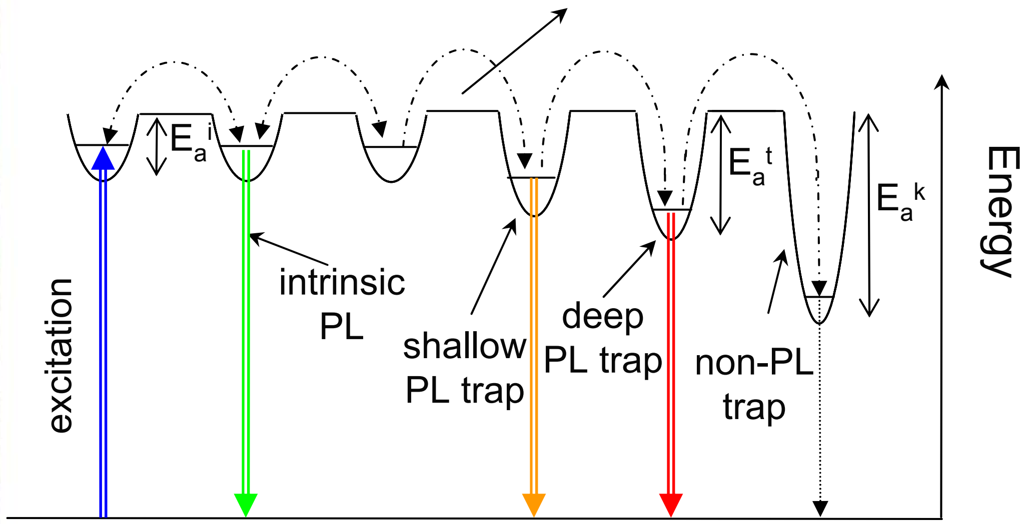

$$\tau^{-1}_{transfer-nr} = p \cdot e^{-\frac{E_a}{KT}}$$

$$w_{DA} \propto |\langle \text{Donor}, \text{Acceptor}^* \,|\, H_{int} \,|\, \text{Donor}^*, \text{Acceptor} \rangle|^2$$

Excitons. PL traps in MnF_2.

Excitation migration and trapping

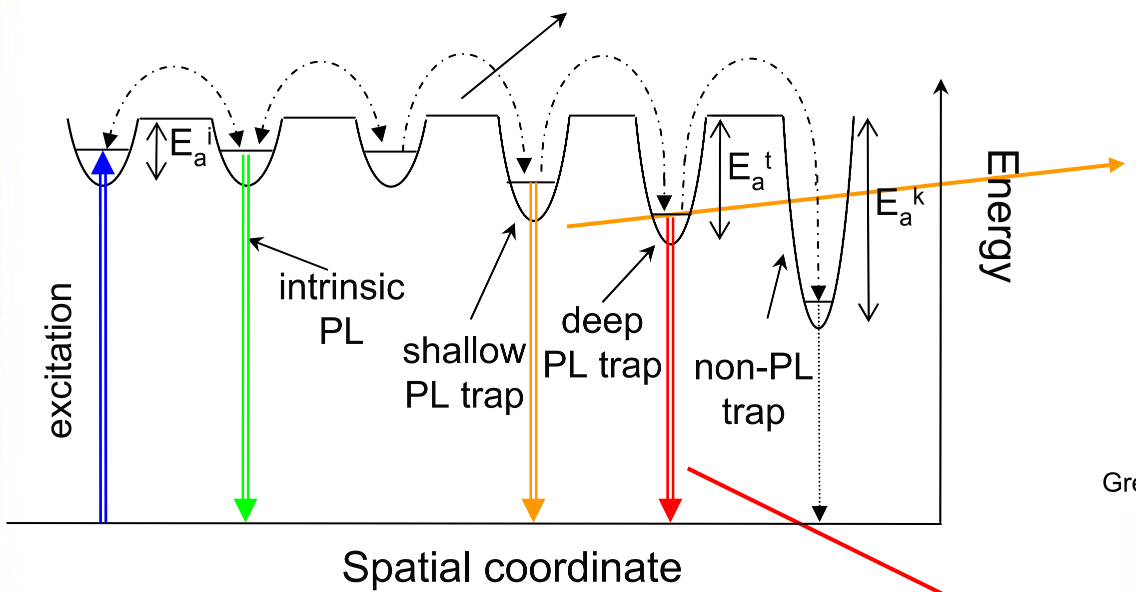

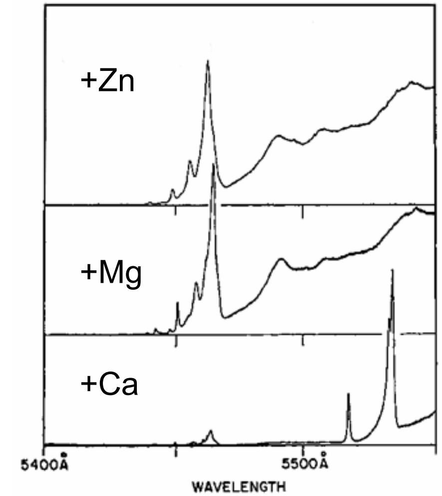

Greene et *al.* Phys Rev. **171**, 600 (1968)

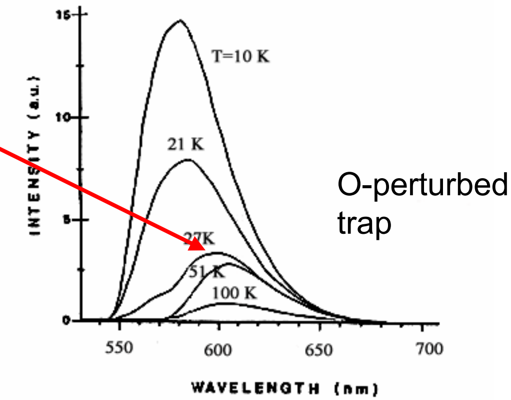

Rodríguez et *al.* J. Physique **46**, 155 (1985)

- Zn^{2+}, Mg^{2+} and Ca^{2+} perturbed Mn^{2+} have been identified as shallow luminescent traps
- Deeper luminescent traps peaking at 2.05 eV are due to oxygen-coordinated Mn^{2+} ions

PL traps in MnF_2.

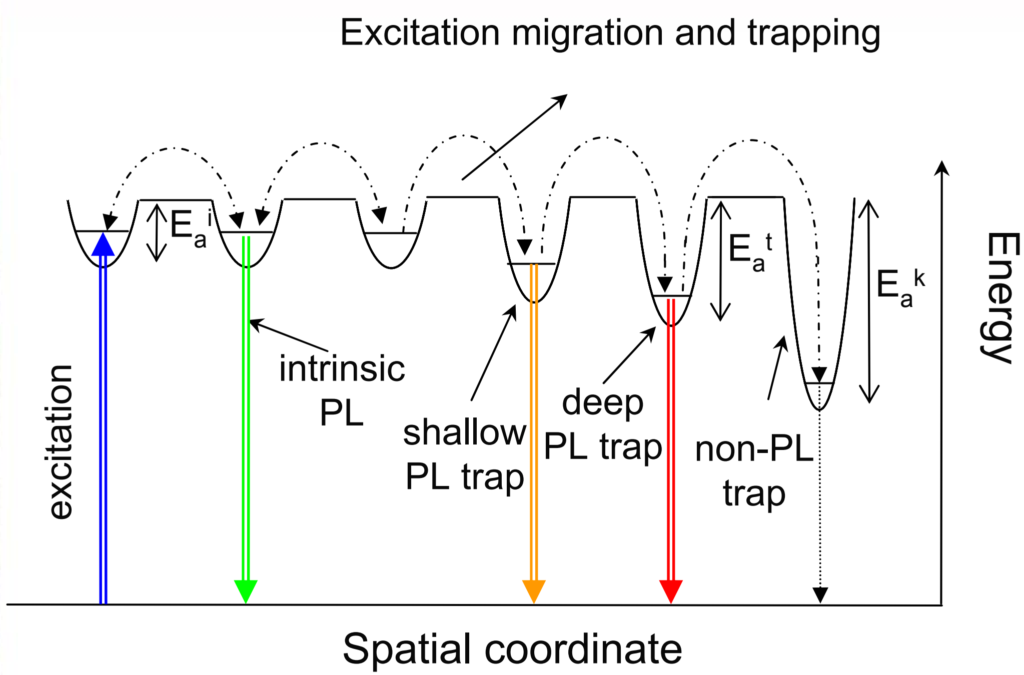

$$w_{DA} \propto |\langle D,A^* \,|\, H_{ex} \,|\, D^*,A \rangle|^2$$

Is it possible to impede transfer to non-radiative de-excitation centers?

1 – Reduce the non-PL impurities (purification)

2 – Avoid transfer (pressure-iduced transformations)

Towards impurity-lean particles: MnF_2 milling.

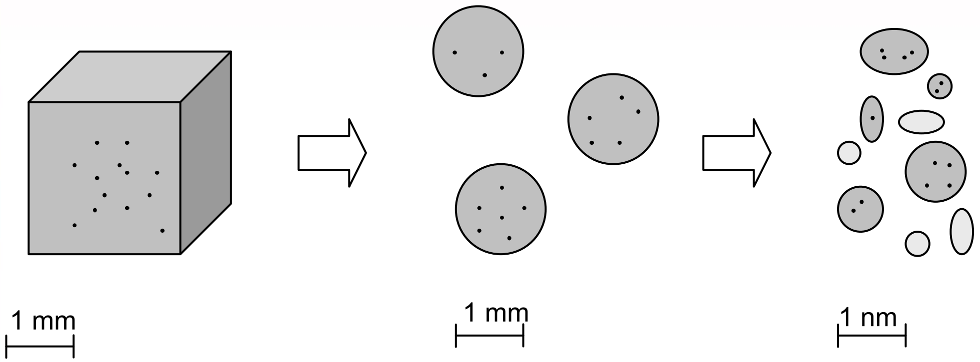

$$P(n) = (1-c)^{N-n} c^n \frac{N!}{(N-n)n!}$$

Decrease in particle size

$\Rightarrow$ impurity-lean particles

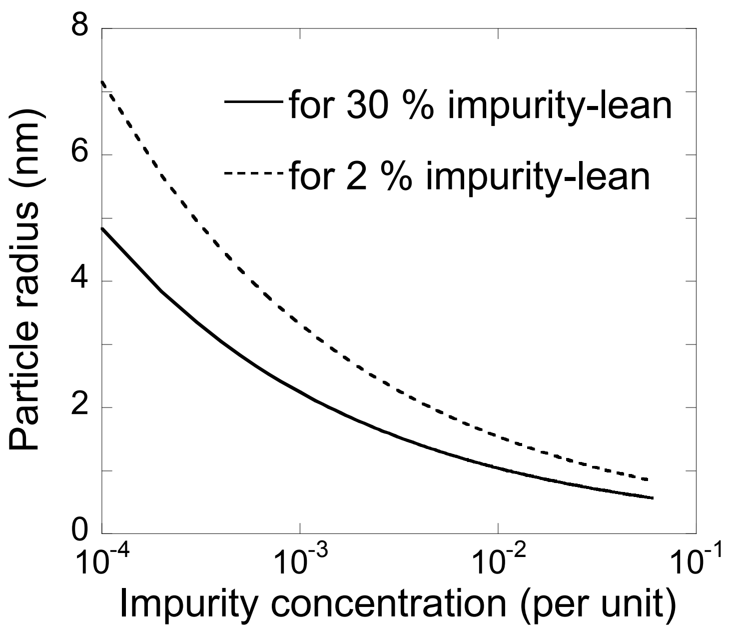

Milled MnF_2 XRD diagrams. Nanoparticles.

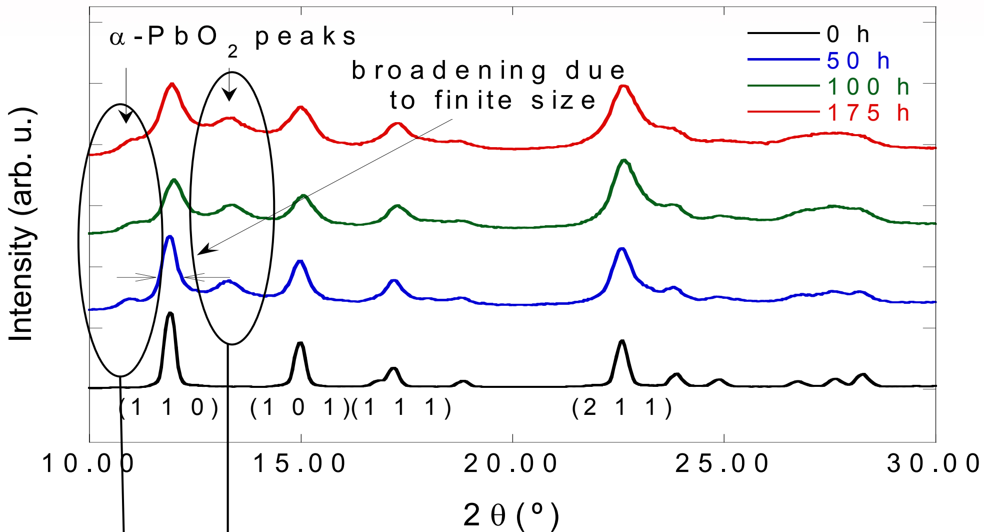

- Grain size reduction

~ 5 nanometers

- Strain broadening

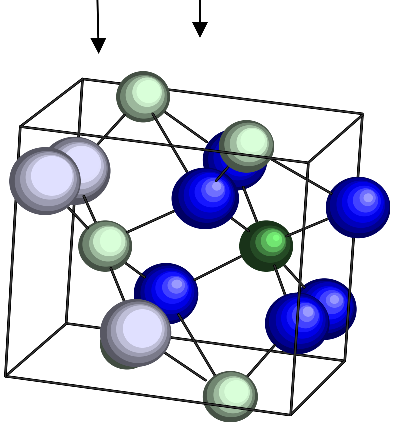

- Milling favours formation of α-PbO_2 phase

F. Dachille and R.Roy, Nature, **186**, 70 (1960)

Optical and IR absorption. Water.

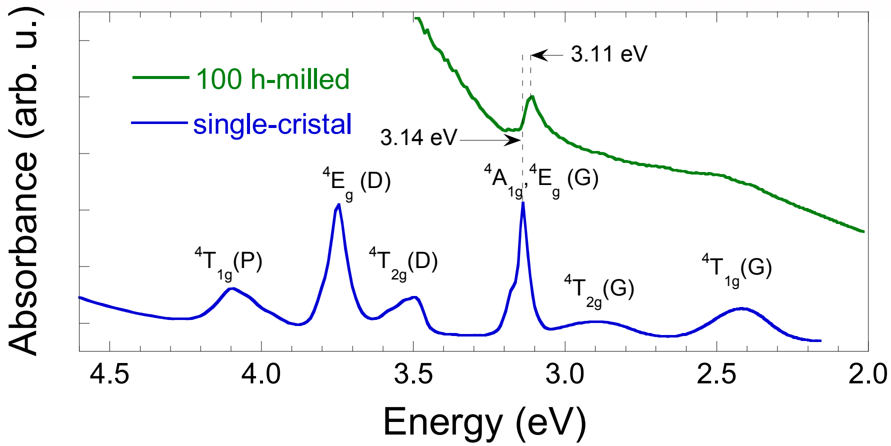

Milled and single crystal absorption spectra are similar

$^4A_{1g}$, ^4E_g slightly redshifted

Optical and IR absorption. Water.

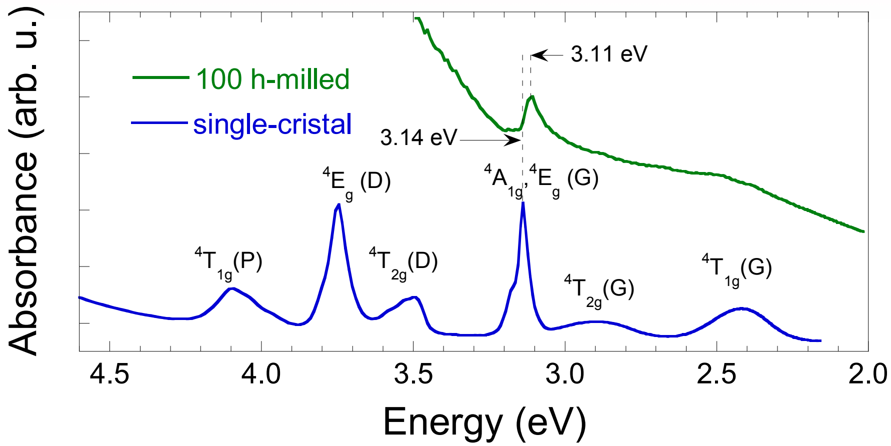

Milled and single crystal absorption spectra are similar

$^4A_{1g}$, ^4E_g slightly redshifted

FTIR: water presence

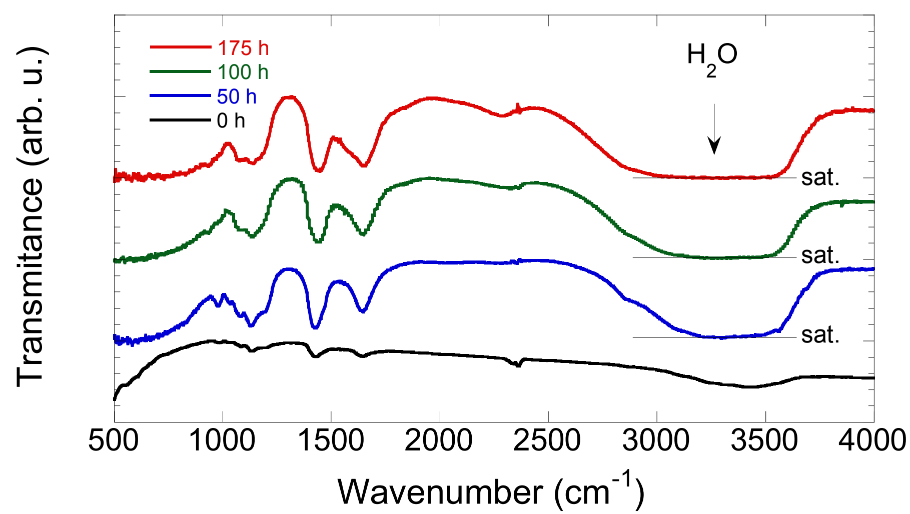

Milled MnF_2 PL spectra at LT.

Milled MnF_2 PL spectra at LT.

Similar results for all milled samples.

New red component.

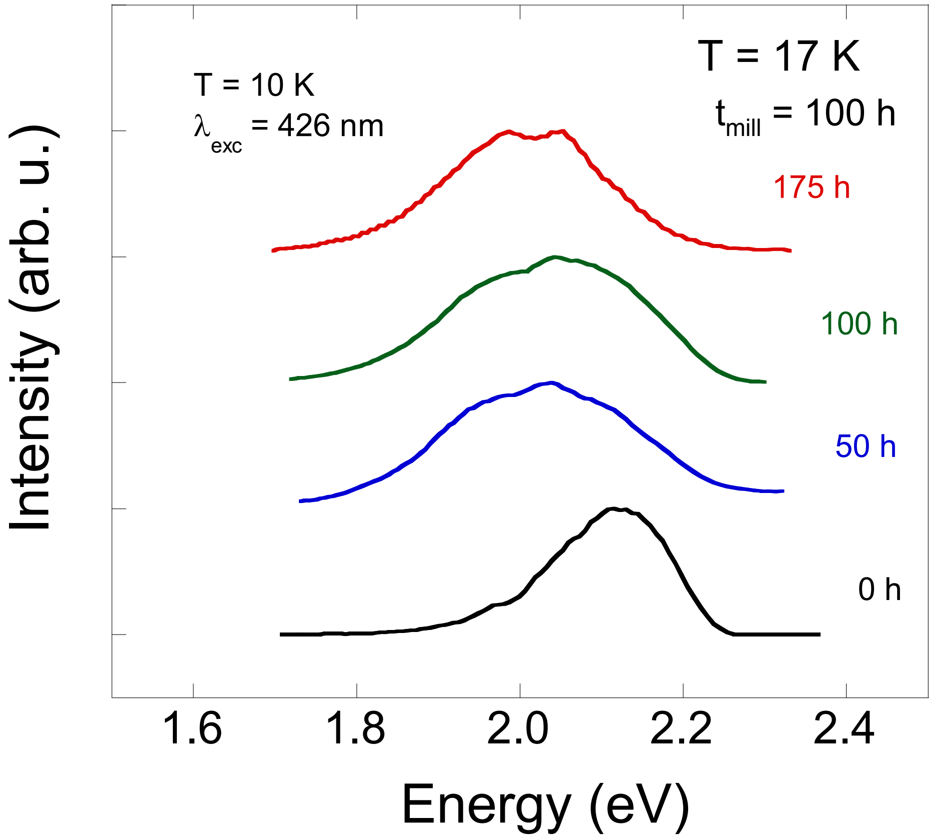

Milled MnF_2 PL spectra at LT.

Similar results for all milled samples.

New red component.

Strongly Inhomogeneous

τ varies along the band

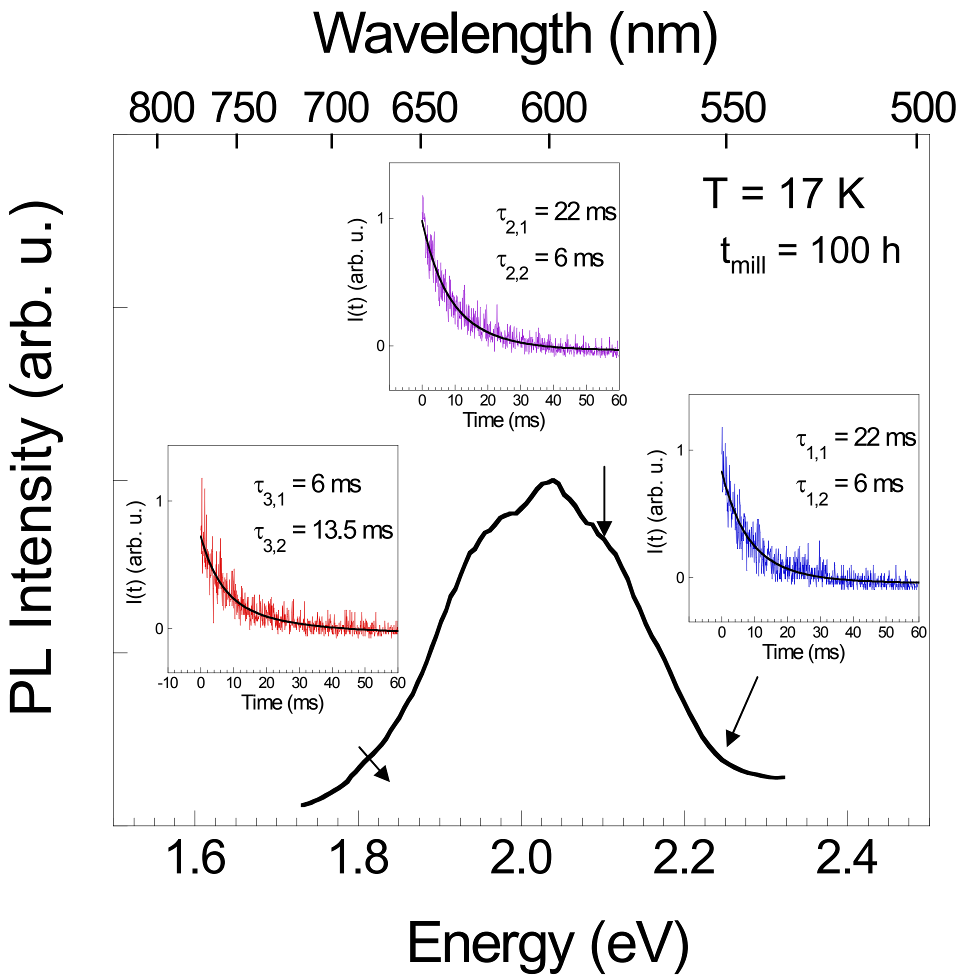

Milled MnF_2 PL spectra at LT.

Similar results for all milled samples.

New red component.

Strongly Inhomogeneous

τ varies along the band

Q-continuous trap distribution

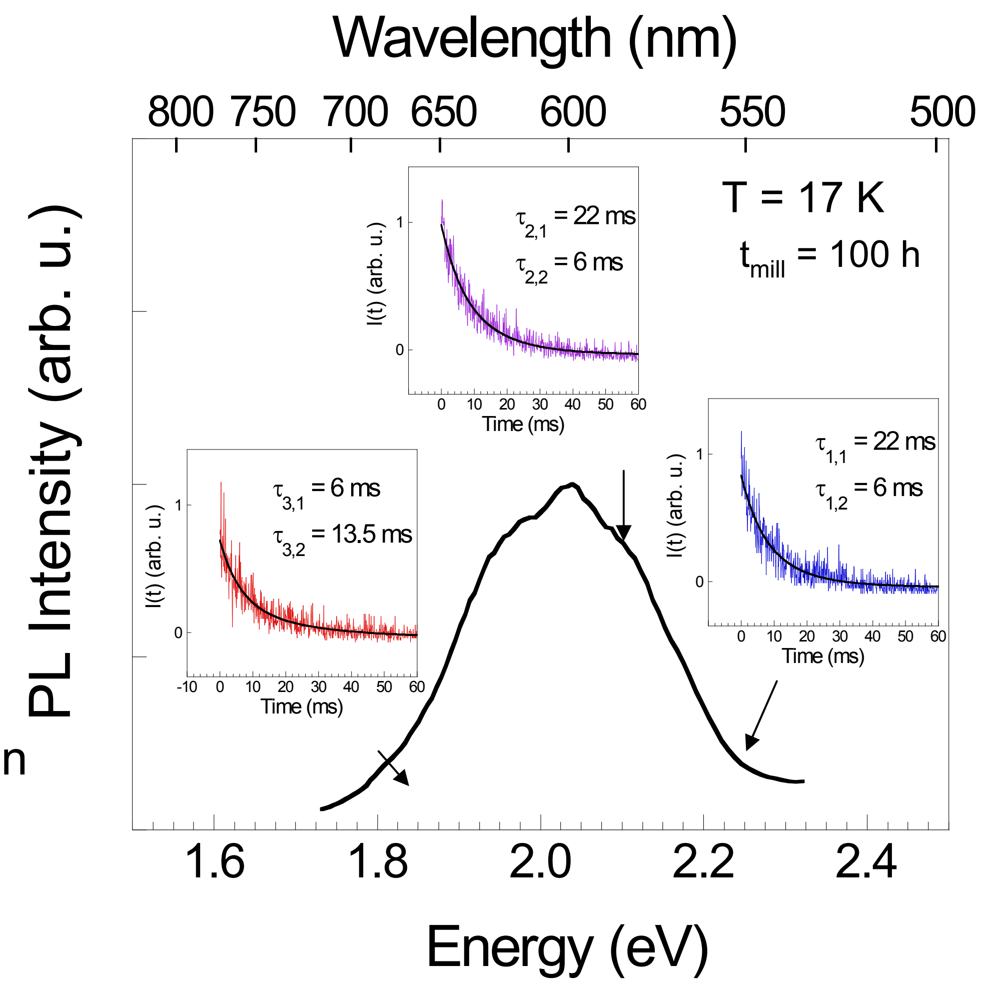

Milled MnF_2 PL spectra at higher T.

Results - MnF_2

Similar results for all milled samples.

New red component.

Strongly Inhomogeneous

τ varies along the band

Q-continuous trap distribution

PL does not remain for T > 200 K

Water may act as non-radiative de-excitation centers.

Milled MnF_2 PL spectra at higher T.

Similar results for all milled samples.

New red component.

Strongly Inhomogeneous

τ varies along the band

Q-continuous trap distribution

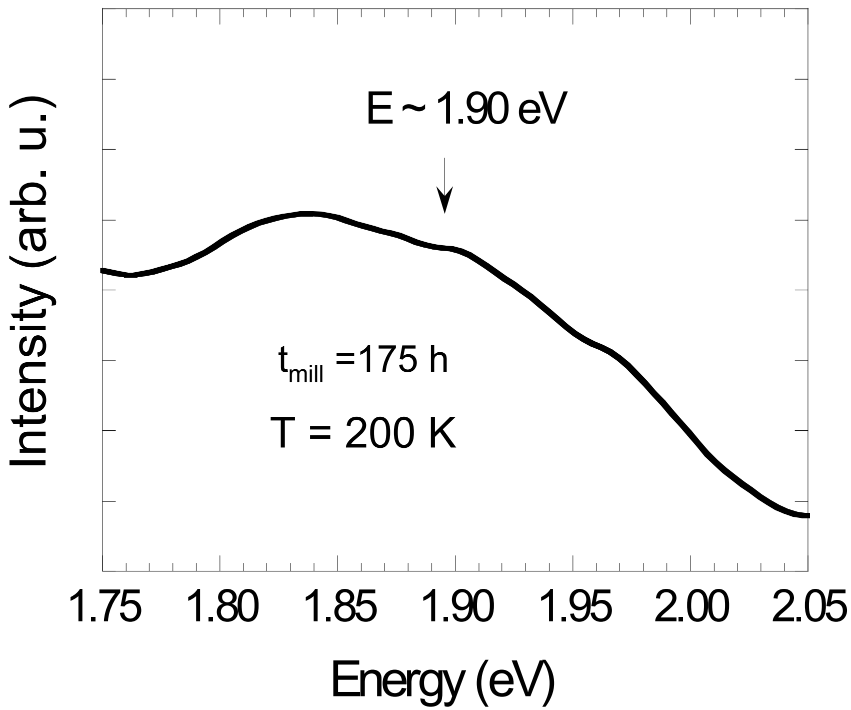

PL does not remain for T > 200 K

$\Delta T_q \sim 90$ K

Water may act as non-radiative de-excitation centers.

Towards stopping transfer: Phase transition sequence.

Towards stopping transfer: Phase transition sequence.

Results - MnF_2

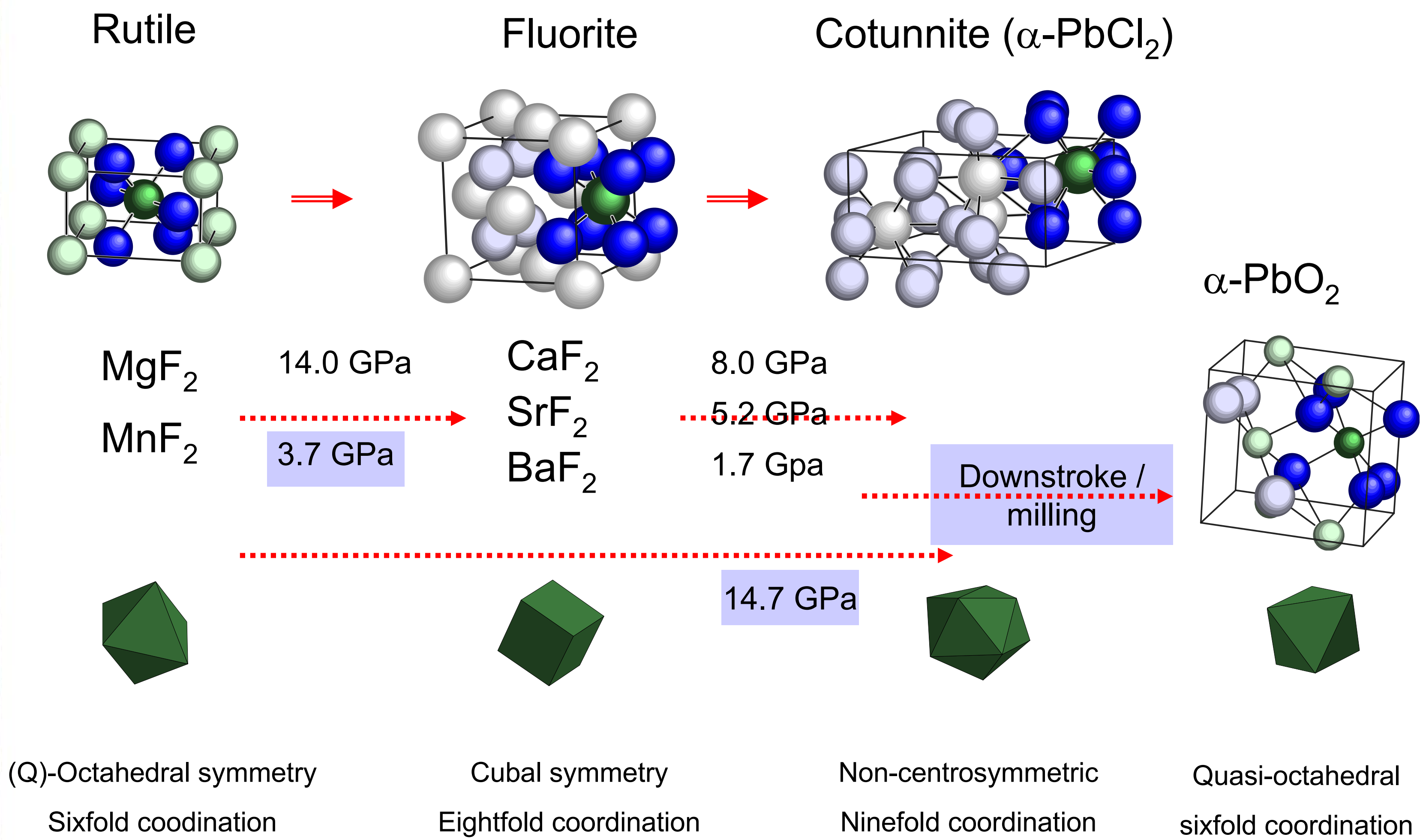

MnF_2 under Pressure: emission spectra.

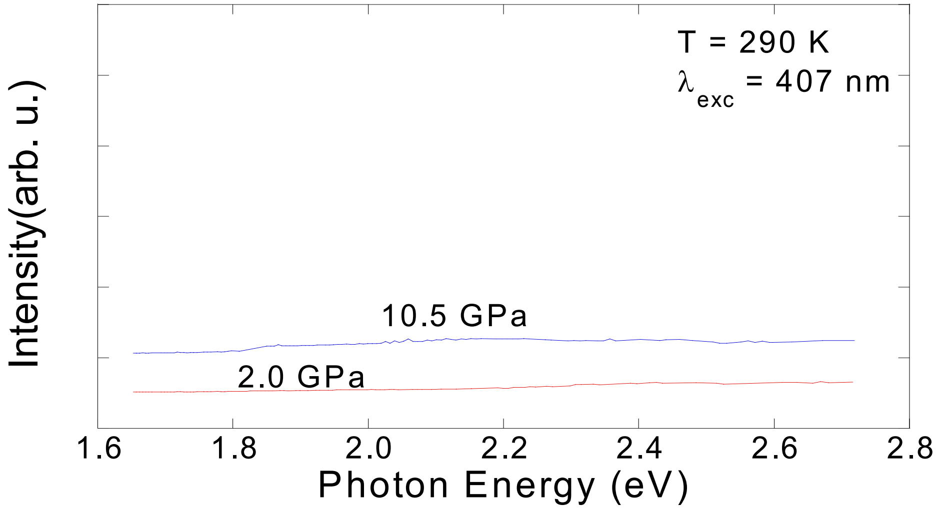

MnF_2 under Pressure: emission spectra.

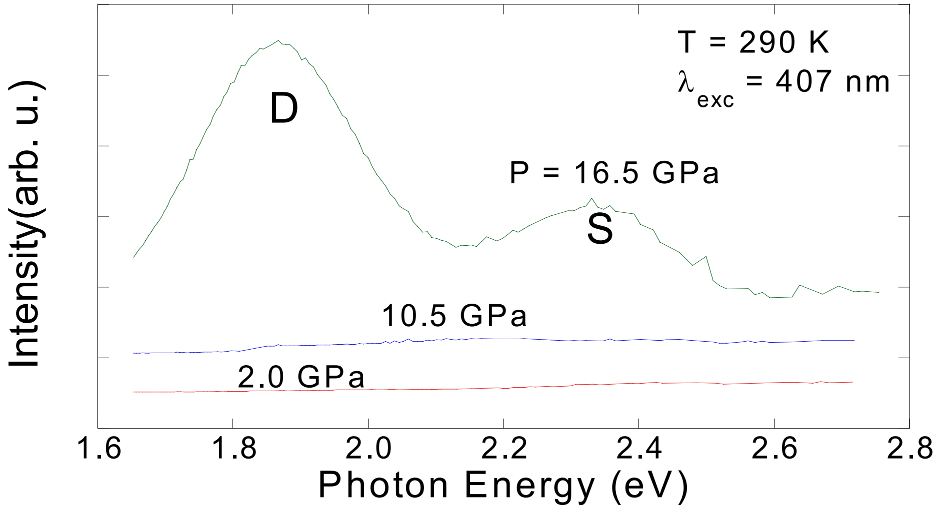

- Two well-resolved bands appear for P > 14.7 GPa

Band S (~ 2.3 eV)

Band D (~ 1.9 eV)

Exciton migration reduction correlates with cotunnite phase!!

MnF_2 under Pressure. Downstroke

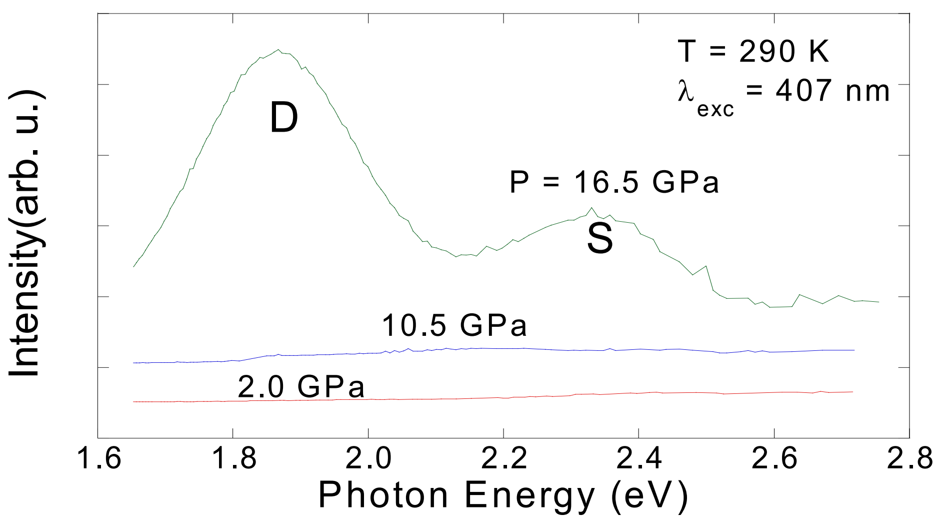

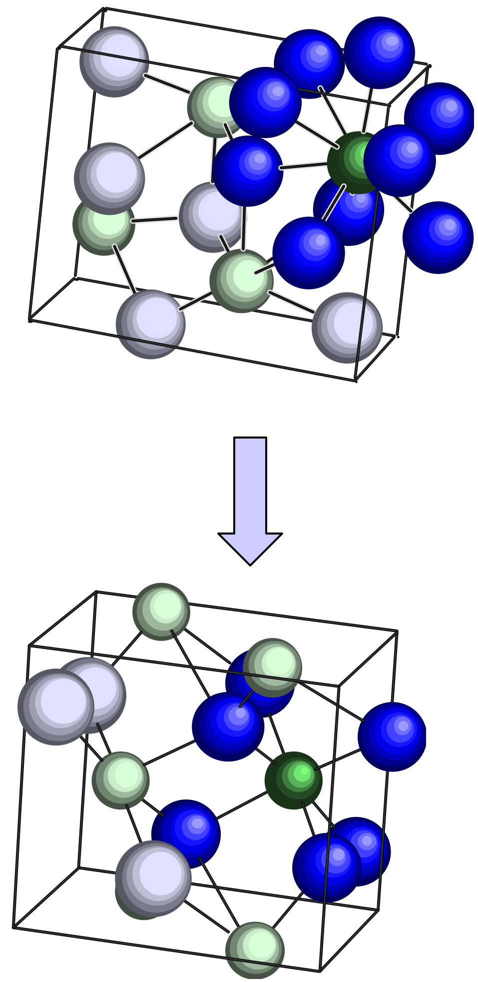

- Luminescence does not remain upon pressure release due to the downstroke α-$PbCl_2$ to α-PbO_2 phase transition at ~ 13.5 GPa.

Time-resolved spectroscopy.

Time-resolved spectroscopy.

Results - MnF_2

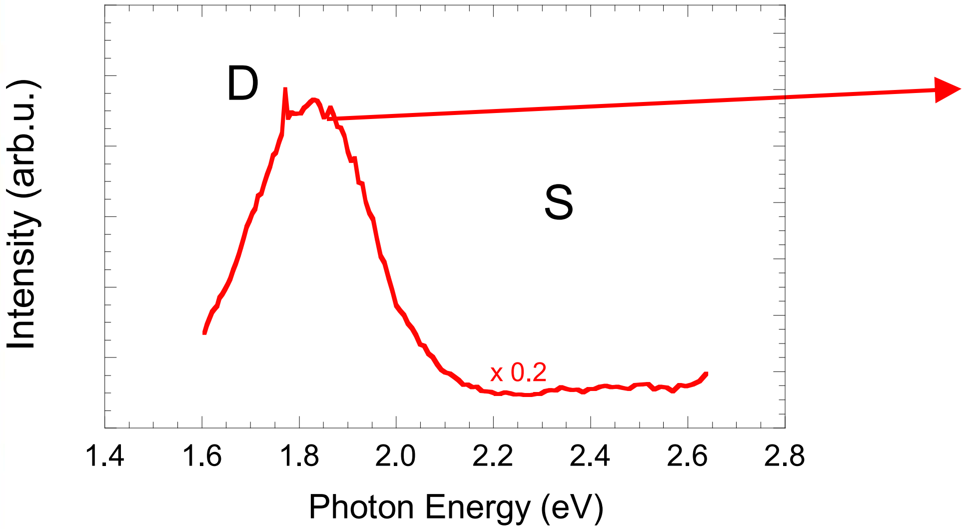

Photon counting **immediately** after laser pulse.

Time-resolved spectroscopy.

Results - MnF_2

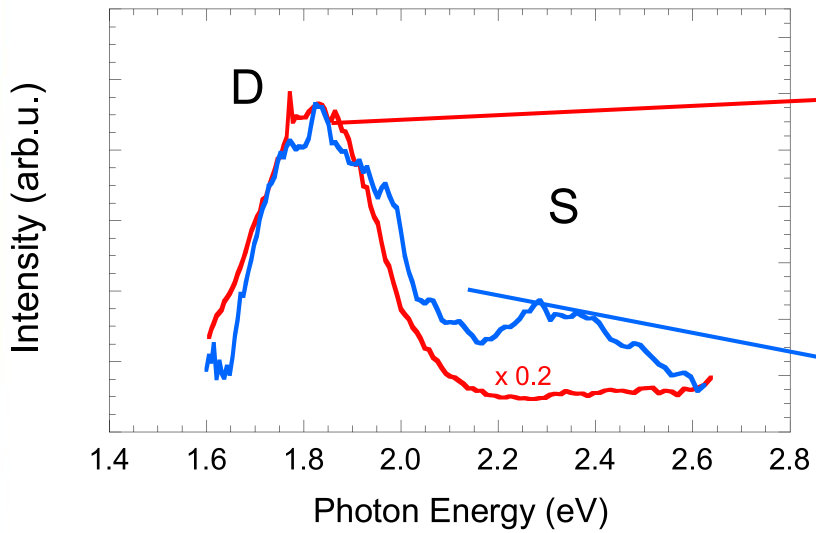

Photon counting **immediately** after laser pulse.

Photon counting **2 ms after** laser pulse delay.

Delayed counting provides an increase in the relative intensity of the S-Band.

$$\tau_S > \tau_D$$

Comparison with CaF_2: Mn^{2+} at HP. Excitation.

Cotunnite Phase

Ninefold coordination

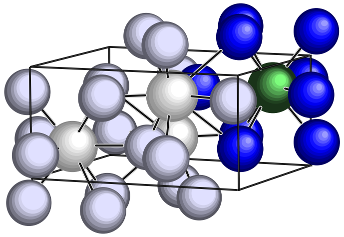

Comparison with CaF_2: Mn^{2+} at HP. Excitation.

Results - MnF_2

Cotunnite Phase

Ninefold coordination

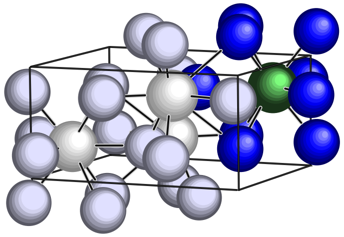

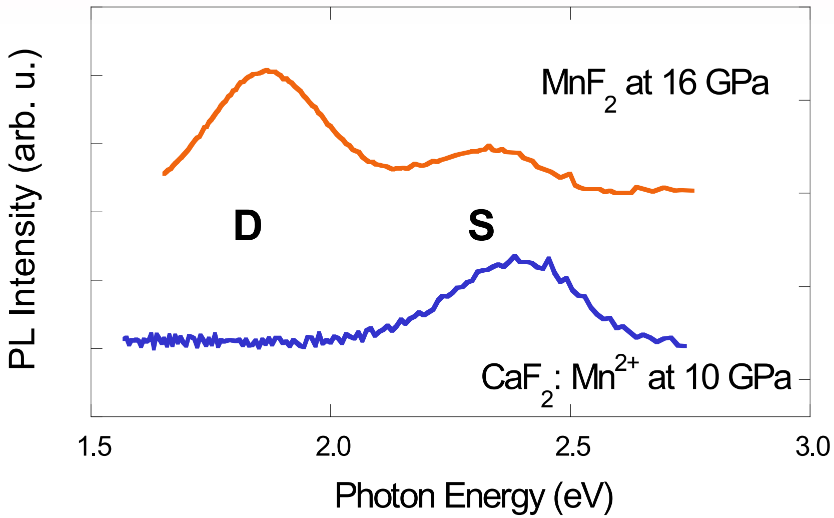

PL lifetime in CaF_2: Mn^{2+} (τ = 14 ms) is bigger than in MnF_2 (4 ms > τ > 2 ms)

Comparison with CaF_2: Mn^{2+} at HP. Excitation.

Cotunnite Phase

Ninefold coordination

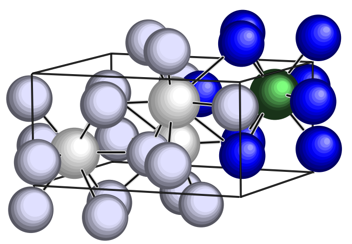

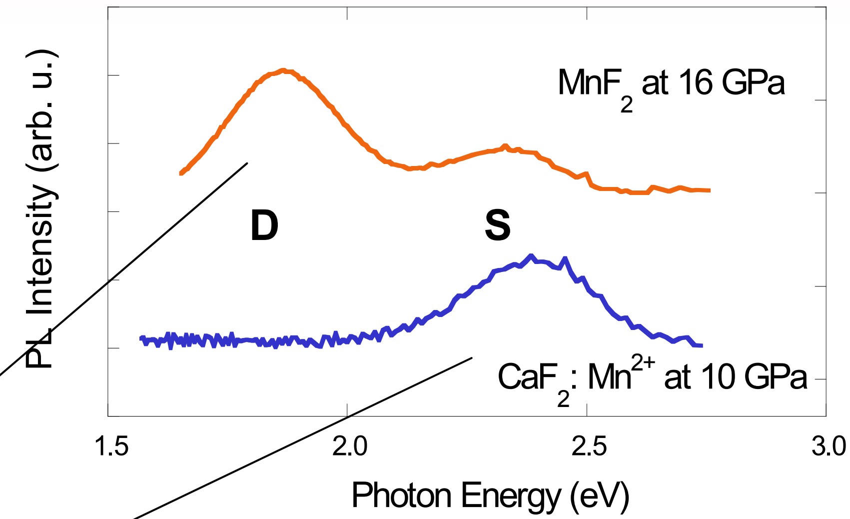

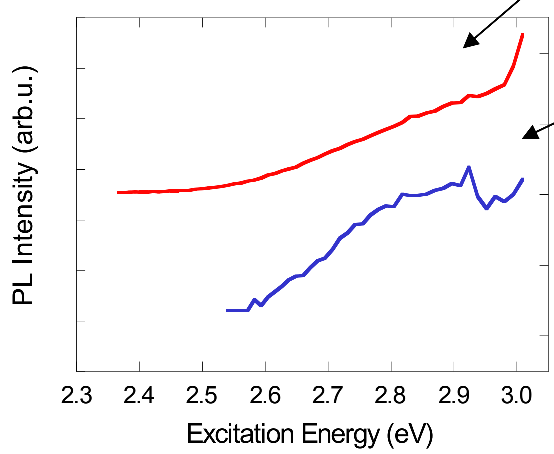

PL lifetime in CaF_2: Mn^{2+} (τ = 14 ms) is bigger than in MnF_2 (4 ms > τ > 2 ms)

Excitation of S-Band in CaF_2: Mn^{2+} is very similar to MnF_2 D-Band excitation.

Time-resolved spectroscopy. Lifetime.

D-Band T = 300 K, P =16 GPa

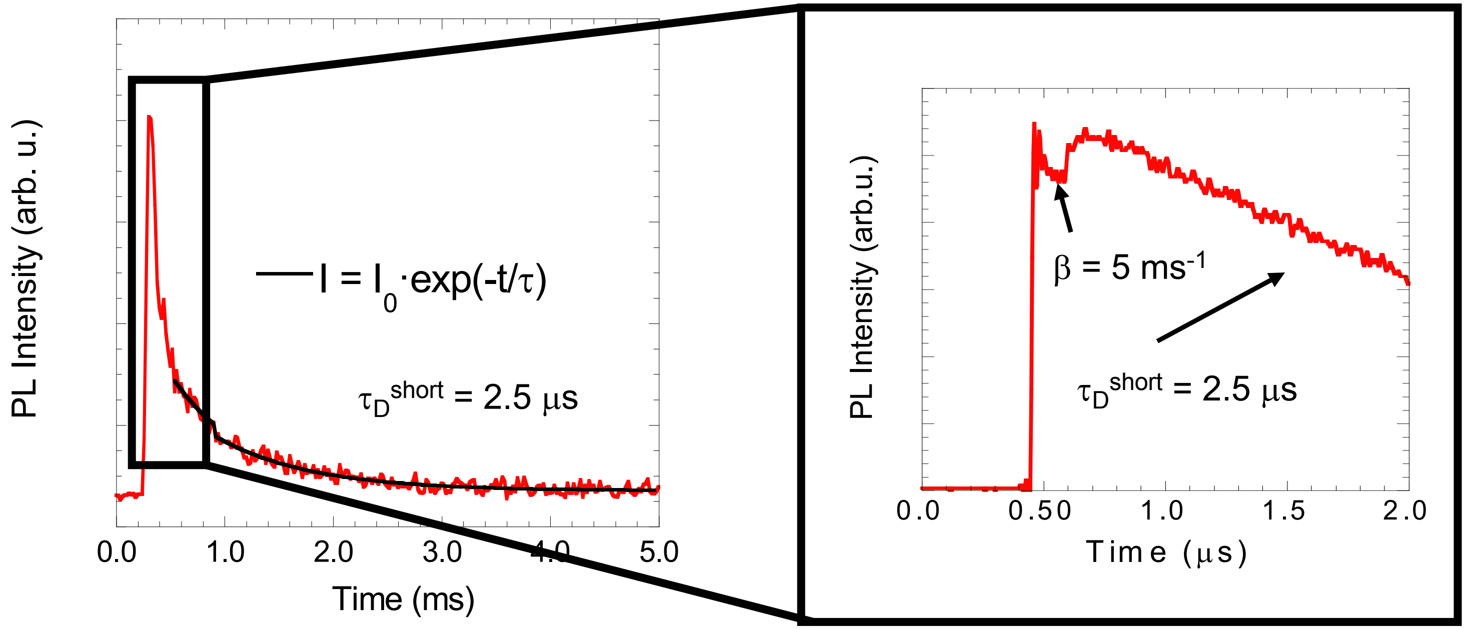

Excitation and I(t) suggest that D-luminescence comes from excitation-transferred centers !!

Excited-States dynamics: model.

S-centers (intrinsic/shallow traps), τ_S = 5 ms

$\tau_0 \Rightarrow$ the Mn^{2+} lifetime without migration

τ_0 = 13 ms in CaF_2: Mn^{2+} in the cotunnite phase

D-centers (deep traps), $\tau_D = \tau_D^{short}$ = 2.5 μs

RN-centers (regular nearby S $\rightarrow$ D)

Non-radiative centers, **K**illing PL

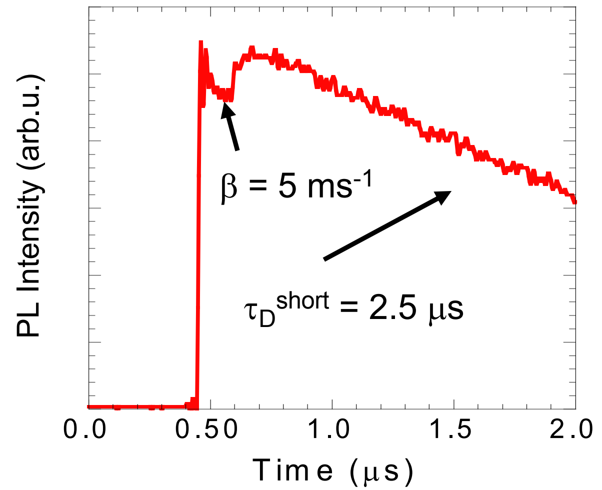

Excited-States dynamics: model.

S-centers (intrinsic/shallow traps), τ_S = 5 ms

$\tau_0 \Rightarrow$ the Mn^{2+} lifetime without migration

τ_0 = 13 ms in CaF_2: Mn^{2+} in the cotunnite phase

D-centers (deep traps), $\tau_D = \tau_D^{short}$ = 2.5 μs

RN-centers (regular nearby S → D)

Non-radiative centers, **K**illing PL

Hernández et al, PRL **99**, 027403 (2007)

$$\frac{dN_D}{dt} = \beta N_{RN} - \tau_D^{-1} N_D$$

$$\frac{dN_{RN}}{dt} = -(\beta + \tau_S^{-1}) N_{RN} + f(t)\gamma N_S$$

$$\frac{dN_S}{dt} = -\tau_S^{-1} N_S = -\left[\tau_0^{-1} + \tau_K^{-1} + \gamma\right] N_S$$

$$\beta >> \gamma$$

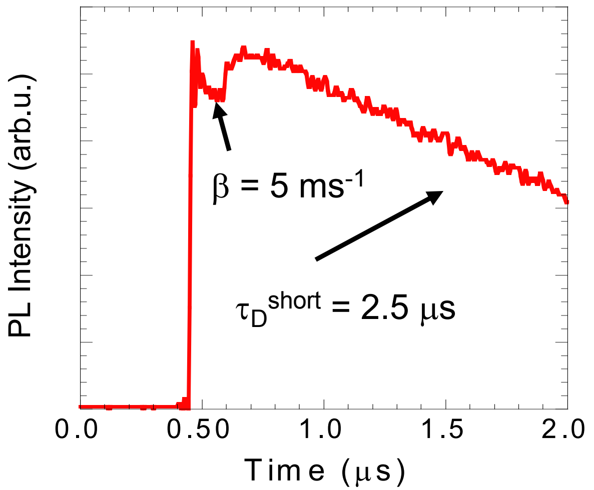

Excited-States dynamics: model.

S-centers (intrinsic/shallow traps), τ_S = 5 ms

$\tau_0 \Rightarrow$ the Mn^{2+} lifetime without migration

τ_0 = 13 ms in CaF_2: Mn^{2+} in the cotunnite phase

D-centers (deep traps), $\tau_D = \tau_D^{short}$ = 2.5 μs

RN-centers (regular nearby S $\rightarrow$ D)

Non-radiative centers, **K**illing PL

Hernández et al, PRL **99**, 027403 (2007)

$$\frac{dN_D}{dt} = \beta N_{RN} - \tau_D^{-1} N_D$$

$$\frac{dN_{RN}}{dt} = -(\beta + \tau_S^{-1}) N_{RN} + f(t)\gamma N_S$$

$$\frac{dN_S}{dt} = -\tau_S^{-1} N_S = -\left[\tau_0^{-1} + \tau_K^{-1} + \gamma\right] N_S$$

$$\beta >> \gamma$$

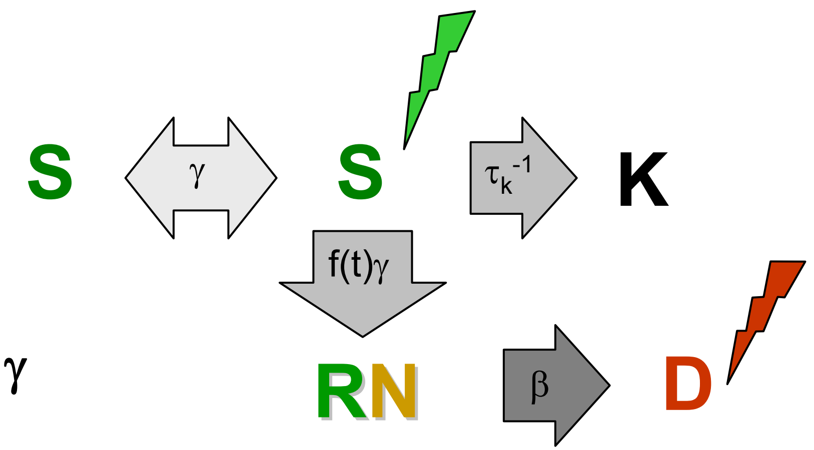

Important exciton migration reduction!!!

Conclusions.

Conclusions.

● $Ca_{1-x}Sr_xF_2$: Mn^{2+} and BaF_2: Mn^{2+} fluorites:

· Non-radiative processes are volume dependent

· A unique expression dependent on T and V describes the series PL

· We have induced PL in non-PL materials of the series at HP

■ A_2BMF_6 : Cr^{3+} fluoroelpasolites

· 10Dq varies as $R_{Cr\text{-}F}^{-3.3}$ instead of $R_{Cr\text{-}F}^{-5}$ } Electronic states mixing

· Stokes shift increases with the Cr local volume } Electronic states mixing

· Rb_2KCrF_6 experiences ESCO upon increasing P

◆ MnF_2

· Milled MnF_2 to nanometric scale increases the PL quenching temperature

· We have not obtained PL at RT at low pressure

☺ We have **induced** and **explained** a novel RT PL at HP in pure Mn^{2+} compound

Acknowledgements.

- High Pressure and Spectroscopy - CITIMAC (University of Cantabria)

  Prof. Fernando Rodriguez

  Dr. Rafael Valiente

  Colleagues and collaborators

- ICMCB (University of Bordeaux, 1)

  Prof. A. Tressaud

- IMPMC (U. Pierre et Marie Curie, Paris VI)

  Dr. J.P. Chervin *et al.*

- Dpt. of Physics (Colorado State University)

  Prof. H.D. Hochheimer

- LPMCN, (U. Claude Bernard, Lyon 1)

  Prof. A. San Miguel *et al.*